TITLE & AUTHORS

HIV-1 Vpr combats the PU.1-driven antiviral response in primary human macrophages.

Maria C. Virgilio[1,2,3], W. Miguel Disbennett[4,5,a], Thomas Chen[5], Jay Lubow[5,b], Joshua D. Welch[2], Kathleen L. Collins[1,3,5,*]

[1]Cellular and Molecular Biology Program, University of Michigan, Ann Arbor, MI, USA

[2]Department of Computational Medicine and Bioinformatics, University of Michigan, Ann Arbor, MI, USA

[3]Department of Internal Medicine, University of Michigan, Ann Arbor, MI, USA\

[4]Post-Baccalaureate Research Education Program (PREP), University of Michigan, Ann Arbor, MI, USA

[5]Department of Microbiology and Immunology, University of Michigan, Ann Arbor, MI, USA

[a]Present location: University of Pennsylvania, Philadelphia, PA, USA

[b]Present location: Fred Hutchinson Cancer Research Center, Seattle, WA, USA

[*] Correspondence: klcollin@umich.edu

SUMMARY

The HIV-1 accessory protein, Vpr, is an enigmatic protein required for efficient spread of HIV from macrophages to T cells, a necessary step for propagation of infection. To illuminate the role of Vpr in HIV-infection of primary macrophages, we used single-cell RNA sequencing to capture the transcriptional changes during an HIV-1 spreading infection plus and minus Vpr. We found that Vpr reprogramed HIV-infected macrophage gene expression by targeting the master transcriptional regulator, PU.1. PU.1 was required for efficient induction of the host innate immune response to HIV, including upregulation of *ISG15*, *LY96,* and *IFI6*. In contrast, we did not observe direct effects of PU.1 on HIV gene transcription. Single cell gene expression analysis also revealed Vpr countered an innate immune response to HIV-infection within bystander macrophages via a PU.1-independent mechanism. The capacity of Vpr to target PU.1 and disrupt the anti-viral response was highly conserved across primate lentiviruses including HIV-2 and several SIVs. By demonstrating how Vpr overcomes a critical early warning system of infection, we identify a crucial reason why Vpr is necessary for HIV infection and spread.

KEYWORDS

Vpr, HIV-1, HIV-2, SIV, PU.1, macrophages, scRNA-seq, interferon, ISG15, TLR

INTRODUCTION

The HIV-1 genome encodes several accessory proteins that counteract innate and adaptive antiviral responses. Although HIV accessory proteins have been widely studied, the role of the Vpr accessory protein has remained enigmatic. Vpr is highly conserved amongst lentiviruses and is necessary for optimal replication in macrophages[1]. Studies using human lymphoid tissue, which is rich in both T cells and macrophages, have found that loss of Vpr decreases virus production but only when the virus strain is capable of efficiently infecting macrophages[1–5]. These studies provide evidence that Vpr enhances infection of macrophages and increases viral burden in tissues containing macrophages. Vpr localizes to the nucleus[6], where it is known to induce G2 cell cycle arrest by targeting a variety of host factors involved in post-replication DNA repair[7–14]. To target these factors, Vpr requires the host protein DCAF1 (also known as Vpr binding protein (VprBP))[15]. Through DCAF1, Vpr interacts with Damaged DNA binding protein 1 (DDB1) as part of the Cul4A E3 ubiquitin ligase complex where host proteins recruited by Vpr can be ubiquitinated, then degraded[16–21]. However, the effects of Vpr on DNA repair and cell cycle arrest do not provide a clear explanation for how Vpr enhances HIV infection of macrophages.

Macrophages are terminally differentiated antigen presenting cells that are critical for many immune functions, including antiviral innate immune responses[22,23]. Macrophage identity is tightly controlled through the timed expression of myeloid transcription factors, particularly PU.1 (Reviewed in [24]). PU.1 is a hematopoietic-specific and ETS family transcription factor that is essential for lymphoid and myeloid development [24–27]. ETS family proteins bind to purine rich DNA domains with a central GGAA/T core consensus[28]. Macrophages require early and continuously high levels of PU.1 expression (Reviewed in [24,25]) to maintain normal functionality. PU.1 regulates many essential macrophage genes including those for cytokine receptors including M-CSF and GM-CSF and the adhesion molecule CD11b. PU.1 also coordinates with other transcription factors such as IRF4 and C/EBPα, and TET methyl cytosine dioxygenase 2 (TET2; also known as ten-eleven translocation 2) to regulate gene expression[24,29–31].

We previously reported that Vpr counteracts accelerated degradation of the HIV Env protein, which occurs in HIV infected macrophages but not T cells. We hypothesized that Vpr disables a macrophage-specific restriction factor that detects and degrades HIV Env. We recently identified this factor as the macrophage mannose receptor (MR), which is highly expressed in

68 macrophages but not T cells[32,33]. MR senses HIV Env via densely packed high mannose
69 residues that serve as pathogen-associated molecular patterns (PAMPs) because they are
70 normally absent from host cellular proteins. MR recognition of HIV Env disrupts infection by
71 promoting lysosomal degradation of Env and Env-containing viral particles [34,35]. Although the
72 canonical targeting of host factors by Vpr involves the binding of Vpr to DCAF1, leading to
73 ubiquitination and degradation via the proteosome, Vpr does not directly interact with MR[34].
74 Instead, Vpr suppresses expression of the MR gene, *MRC1*[34]. Here, we examine the
75 mechanism by which Vpr suppresses the expression of *MRC1* and demonstrate that Vpr
76 additionally exerts suppressive effects on other important genes in macrophages to enhance
77 virion assembly and spread.
78
79 To accomplish this goal, we employed single-cell RNA sequencing (scRNA-seq) of primary
80 human macrophages infected with infectious wild type or Vpr-null HIV. Single-cell resolution
81 allowed us to distinguish the effects of Vpr on both infected and virally exposed, uninfected cells
82 in the same culture. Within infected cells, Vpr selectively downregulated genes controlled by the
83 macrophage-selective transcription factor, PU.1. By targeting PU.1, Vpr systemically disrupted
84 several antiviral factors, including *MRC1,* that would otherwise restrict HIV infection and spread.
85 Interestingly, we also identified PU.1 as the transcription factor responsible for partnering with
86 TET2 to control expression of *IFITM3,* a previously reported target of Vpr that is also capable of
87 disrupting Env function[36]. Comparing the expression of antiviral-response genes between
88 infected cells and virus-exposed uninfected bystander cells in the same culture, we discovered
89 that Vpr caused a systemic reduction in genes implicated in Toll-like receptor and Type I
90 interferon (IFN-I) signaling that affected all the cells in the culture. Thus, we provide a systems
91 level explanation for the positive effect of Vpr on HIV spread in macrophages.
92
93 Finally, we found that Vpr-mediated downmodulation of PU.1-regulated gene expression is
94 mediated by direct protein-protein interaction between Vpr and PU.1, resulting in accelerated
95 proteasomal degradation of PU.1. This activity of Vpr is conserved among all HIV-1 molecular
96 clones tested as well as HIV-2 and SIV. Remarkably, both the interaction between PU.1 and Vpr
97 as well PU.1's subsequent degradation, require the Vpr interacting protein, DCAF1. Intriguingly,
98 the PU.1 transcriptional co-factor, TET2, is co-recruited with PU.1 to DCAF1 by Vpr, which
99 aligns our results with other reports that Vpr targets TET2[36,37]. Altogether, our data support a
100 model in which Vpr promotes HIV spread via systemic detrimental effects on the host innate
101 antiviral response to infection.

RESULTS

Single-cell RNA sequencing of HIV-1 infected MDMs reveals Vpr-dependent transcriptional changes. Vpr is known to counteract a number of host factors, primarily those implicated in DNA repair and restriction of HIV Env [34,36]. Recently we demonstrated Vpr decreases transcriptional expression of the host restriction factor, mannose receptor (*MRC1*), which we hypothesize results from Vpr targeting a macrophage-specific transcription factor (Figure 1A). To identify the transcription factor targeted by Vpr, we undertook an unbiased approach to characterize the genome-wide effects of HIV-1 Vpr in monocyte derived macrophages (MDMs). For these studies, we used an infectious HIV molecular clone (89.6) plus or minus an intact *vpr* gene (Figure 1B). We infected primary human $CD14^{+}$ MDMs from three independent healthy donors and allowed the infection to spread for 10 days before harvesting cells (uninfected, 89.6^{wt} or $89.6^{\Delta vpr}$ infected) and prepared them for single-cell gene expression analysis (Figure 1C). LIGER (Linked Inference of Genomic Experimental Relationships) [38] was used to integrate all nine data sets. LIGER enabled us to identify shared cell profiles across donors while reducing sample-specific differences. Uniform Manifold Approximation and Projection (UMAP) visualization of all donor sets showed no significant donor or batch-specific differences amongst the samples (Figure 1D). Integration of virus-treated cells revealed a relatively homogeneous population (Figure 1E, left), with 89.6^{wt} and $89.6^{\Delta vpr}$-exposed cells evenly dispersed throughout the clusters (Figure 1E, center).

To separate the bona fide infected cells from bystander cells, we computationally segregated cells into a subset that expressed both *tat* and *gag* transcripts from those that expressed neither (Figure 1E, right, designated “Infected”). The proportion of infected cells identified by this analysis was like that found by the standard method of identifying infected cells by intracellular Gag staining and detection by flow cytometry (Supplemental Table 1). A comparison of gene expression profiles in cells with and without Vpr revealed that Vpr expression boosted HIV gene expression as previously reported[39] and caused a significant transcriptional shift in host gene expression (Figure 1F). Using a Wilcoxon rank-sum test and false discovery rate correction, we identified 3150 genes with statistically significant two-fold or greater differential expression between 89.6^{wt} and $89.6^{\Delta vpr}$-infected cells.

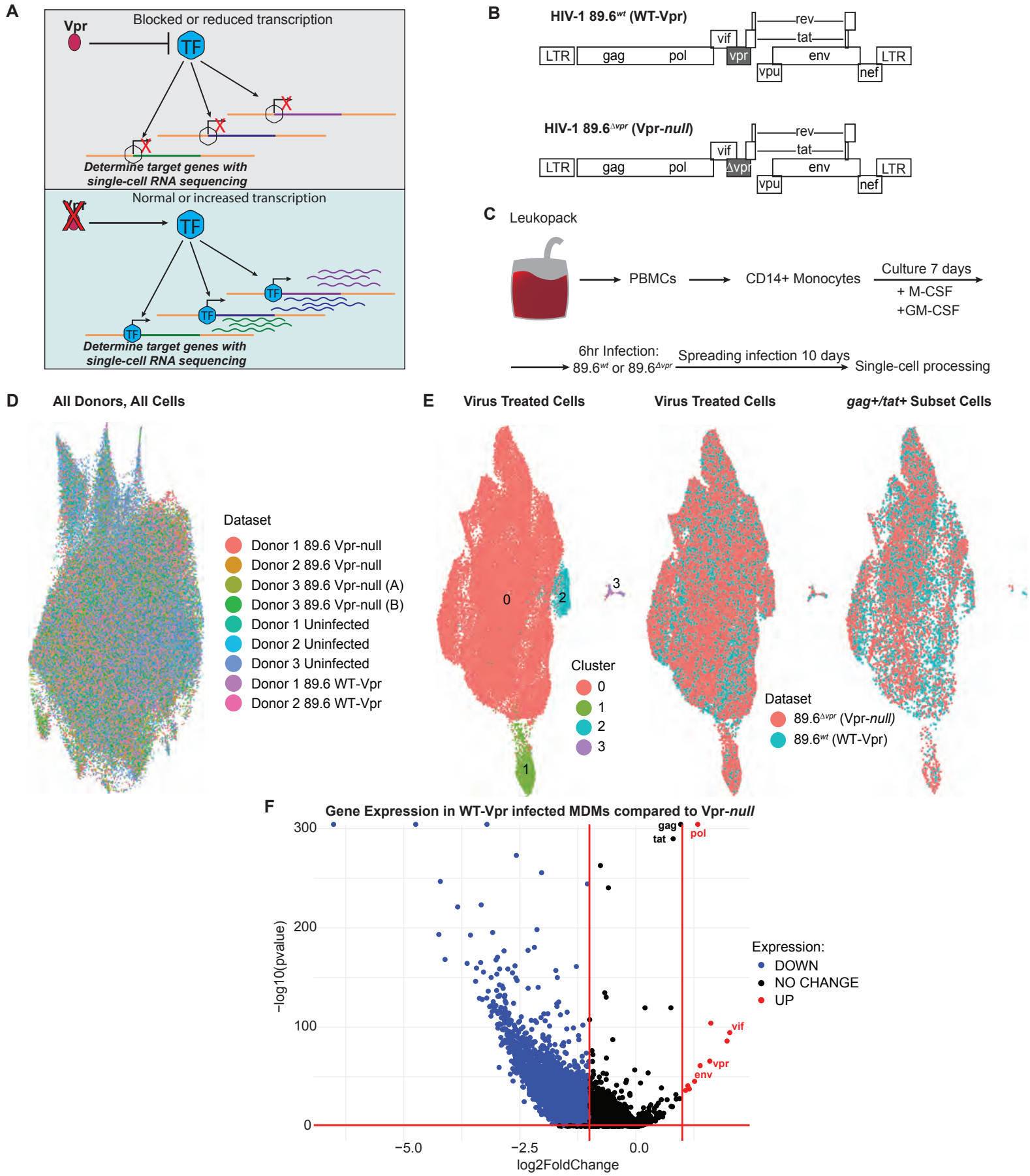

Figure 1. Single-cell RNA sequencing of HIV-1 infected MDMs reveals Vpr-dependent transcriptional changes. (A) Schematic diagram illustrating the objective of single-cell RNA sequencing; the identification of Vpr-targeted transcription factor(s) in HIV infected primary macrophages. (B) Genome maps for full-length 89.6^{wt} HIV-1 (top) and the same viral genome with a premature stop-codon in *vpr* (bottom). (C) Experimental setup for the generation of the scRNA-seq datasets. (D) UMAP representation of LIGER-integrated scRNA-seq data from MDM samples treated as shown in (C) and listed in Dataset. (E) UMAP representations of LIGER-integrated scRNA-seq data from MDMs treated as indicated. (E, Right) Bona fide infected cells were identified based on expression of HIV *tat* and *gag*. (E, left) Colors indicate individual clusters. Cluster 0 = pro-inflammatory macrophages, Cluster 1 = cycling cells, Cluster 2 = dying cells, Cluster 3 = pro-inflammatory macrophages. (E, center and right) cells colored according to whether they were exposed to 89.6 WT-Vpr virus (blue) or Vpr-*null* virus (pink). (F) Volcano plot of differentially expressed genes from HIV 89.6^{wt} verses 89.6$^{\Delta vpr}$ infected MDMs from (E) as determined by Wilcoxin Rank Sum. Significance determined as greater than 1 log2 fold change and false discovery rate adjusted p-value of $p < 0.05$ (red-bars). Blue colored genes indicate genes less highly expressed in HIV 89.6^{wt} verses 89.6$^{\Delta vpr}$ infected MDMs, Red colored genes indicate genes more highly expressed, and black colored genes indicate no significant difference between datasets.

135 **Vpr-repressed genes in MDMs include targets of the transcription factor, PU.1.**
136 To identify the transcription factor(s) targeted by Vpr, we used the DNA motif identification
137 software, HOMER (Hypergeometric Optimization of Motif EnRichment), to scan for common
138 transcription factor binding motifs in the promoters of genes downregulated in the presence of
139 Vpr. Our analysis revealed several candidate transcription factors (TFs) and TF-binding families,
140 including many members of the ETS family of TFs (Supplemental Figure 1A). However, only
141 PU.1 (encoded by the gene *SPI1*) was highly expressed in our data sets (Figure 2B). Moreover,
142 PU.1 appeared twice in the list – as both a member of the ETS family and as a co-factor in the
143 ETS/IRF (Interferon Regulatory Factor) family of transcription factors, a relationship that is well
144 documented[29] (Figure 2A). PU.1 is the master myeloid transcription factor (Reviewed in [26,40,41]).
145 It is required for terminal differentiation of macrophages and is necessary to maintain
146 macrophage immune function [24]. From the list of most downregulated genes in Vpr-expressing
147 MDMs, HOMER identified 316 genes with a PU.1 binding motif in their promoter and 670 PU.1-
148 IRF co-regulated genes, for a combined 840 distinct PU.1-regulated genes identified (Figure 2C,
149 E). One of the genes identified with a PU.1 binding motif was interferon induced transmembrane
150 protein 3 (*IFITM3)*. IFITM3 was previously identified as an important host restriction factor that is
151 similar to mannose receptor, in that IFITM3 targets HIV Env and has reduced gene expression
152 (by reverse transcription quantitative PCR (RT-qPCR)) in the presence of Vpr in HIV-infected
153 MDMs[36]. Gene ontology analysis of the 840 genes targeted by PU.1 revealed that they are
154 enriched for regulation of the immune system and defense response (Figure 2D).
155
156 Because we had previously demonstrated that the gene encoding mannose receptor (*MRC1*)
157 was transcriptionally downmodulated approximately two-fold by Vpr in HIV infected primary
158 human macrophages using RT-qPCR[34], we examined our data set to specifically identify *MRC1*
159 transcripts. In the scRNA-seq data set shown here, we identified a Vpr-dependent change in
160 *MRC1* transcripts (log2FC = 0.932) that is statistically significant (false-discovery rate corrected
161 Wilcoxon rank-sum p-value = 0.002) but fell just below our arbitrary cutoff of a two-fold change
162 (Figures 1F, 2C). Consistent with the pattern we observed for other Vpr-suppressed genes, we
163 identified several PU.1 binding sites in the promoter region of *MRC1* (Supplemental Figure 2)
164 when we manually scanned for PU.1 binding motifs, some of which have been previously
165 described[42]. While the effect of Vpr on *MRC1* expression is relatively small, it combines
166 synergistically with HIV Nef-dependent disruption of MR trafficking to reverse mannose
167 receptor-dependent lysosomal degradation of Env in HIV infected primary macrophages[34].
168

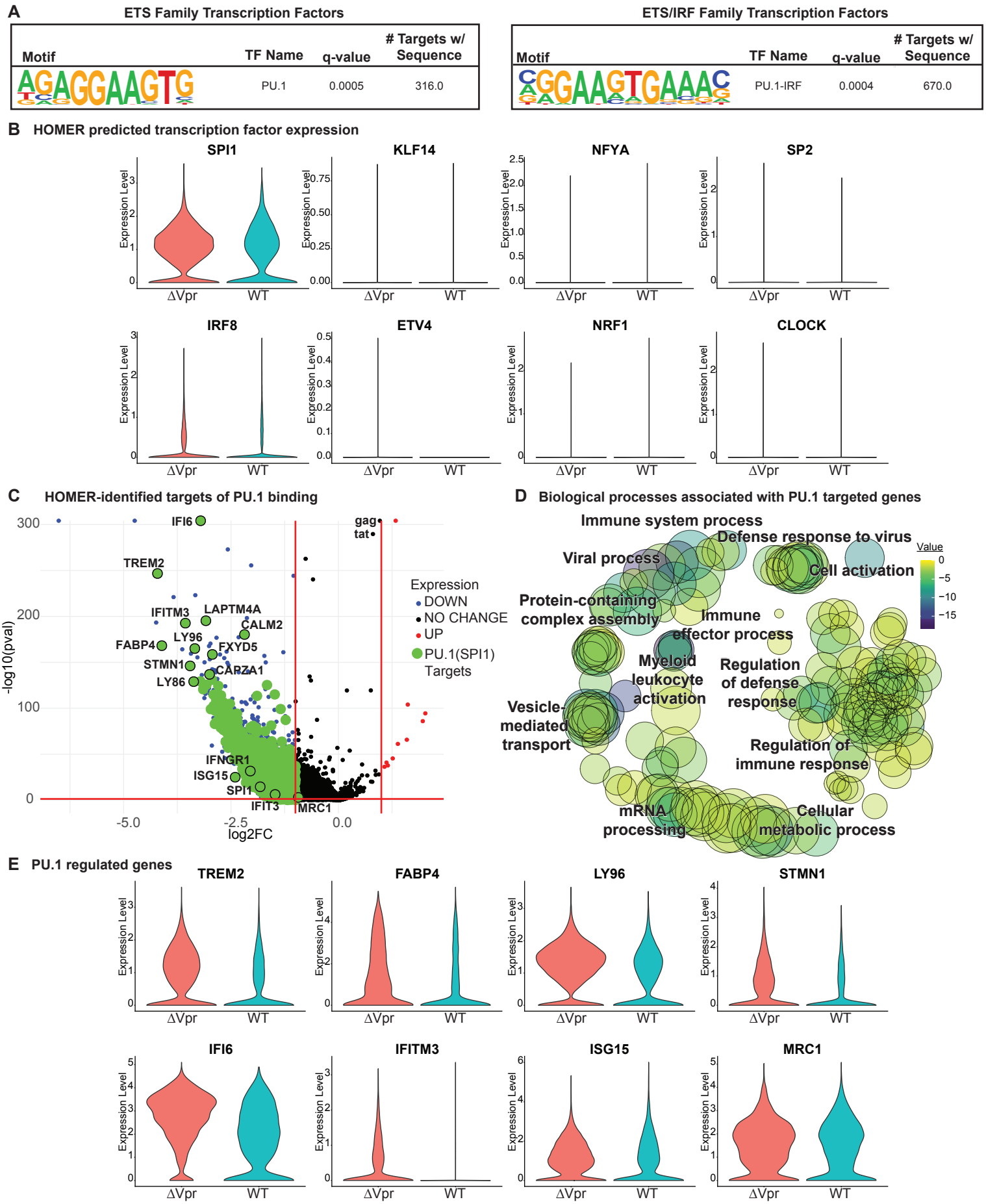

Figure 2. Vpr downmodulates PU.1-dependent transcription. (A) PU.1 motifs identified by HOMER as present in the promoters of Vpr-downmodulated genes (Figure 1E, Blue). (B) Violin plots displaying RNA abundance of the indicated transcription factor genes in MDMs infected with the indicated virus. (C) Volcano plot as in Figure 1E except that genes containing a PU.1 or PU.1-IRF binding motif in their promoter region are highlighted in green (See also Supplemental Figure 2). (D) Biological processes associated with the PU.1 targeted genes from (B). Size of circle indicates the relative number of GO terms with the process. FDR adjusted q-values associated with GO terms as indicated by the color. (E) Violin plots displaying RNA abundance of the indicated genes in MDMs infected with the indicated virus. HIV-1 89.6^{wt} (WT); HIV-1 89.6$^{\Delta vpr}$ (ΔVpr).

169 **Vpr suppresses PU.1 regulated genes implicated in Toll-like receptor and IFN-I**
170 **responses.**
171 PU.1 regulated genes that are downmodulated in Vpr expressing cells include several factors
172 implicated in Toll-like receptor (TLR) signaling pathways (Figure 3A). TLRs are evolutionarily
173 conserved, pattern recognition receptors (PRRs) that recognize PAMPs ([43–45]), including HIV. To
174 determine whether these effects of Vpr are restricted to infected cells within the culture, we
175 compared gene expression profiles amongst all the sample types collected from our single-cell
176 analysis: uninfected (virus naive), 89.6^{wt} and $89.6^{\Delta vpr}$-infected, and 89.6^{wt} and $89.6^{\Delta vpr}$ virally
177 exposed but uninfected (bystander) cells. This was accomplished by computationally
178 segregating cells into subsets that expressed both *tat* and *gag* transcripts from those that were
179 virally exposed but appeared uninfected (*tat* and *gag*-negative) (Figure 3B).
180
181 As expected, expression of genes involved in the TLR-mediated IFN-I response to infection,
182 including Interferon Stimulated Gene 15 (*ISG15),* which is upregulated in response to IFN-I and
183 TLR-signaling (Reviewed in [46,47]), *LY96, and* interferon inducible protein-6 (*IFI6)* (PU.1-IRF
184 regulated genes) and *IFITM3* was very low in uninfected, unexposed cells (Figure 3C). In
185 contrast, each of these genes was upregulated in cells from HIV treated primary macrophage
186 cultures (Figure 3C). As discussed above, Vpr counteracted upregulation of this anti-viral
187 response in infected cells (Figure 2C, E and Figure 3C). In addition, we were surprised to find
188 many of these genes upregulated in bystander cells as well (Figure 3C) and that Vpr limited
189 their induction. For example, we found that *ISG15*, was more highly expressed in $89.6^{\Delta vpr}$
190 bystander cells compared to 89.6^{wt}-exposed bystander cells. Similar observations were made
191 for *LY96*, *IFI6*, and *IFITM3*. Interestingly, the protein product for *LY96* is myeloid differentiation 2
192 (MD2) which is required for TLR4 ligand-induced activation at the cell surface[48,49]. By
193 comparison, other subsets of genes, including *SPI1* and *MRC1* were primarily downmodulated
194 in the infected subset and either not at all in the bystander cells or to a lesser extent than their
195 infected counterparts (Figure 3B).
196
197 **PU.1 protein levels decrease in the presence of Vpr.**
198 Vpr is known to act as an adaptor protein that links host proteins to the Cul4A E3 ubiquitin
199 ligase complex for ubiquitylation and degradation[16,17]. Thus, we hypothesized that Vpr
200 downregulates PU.1-regulated genes in infected cells by targeting PU.1 for proteasomal
201 degradation. To test our hypothesis, we first investigated whether Vpr reduced PU.1 protein
202 levels in infected MDMs. We treated macrophages with a VSV-G envelope-pseudotyped

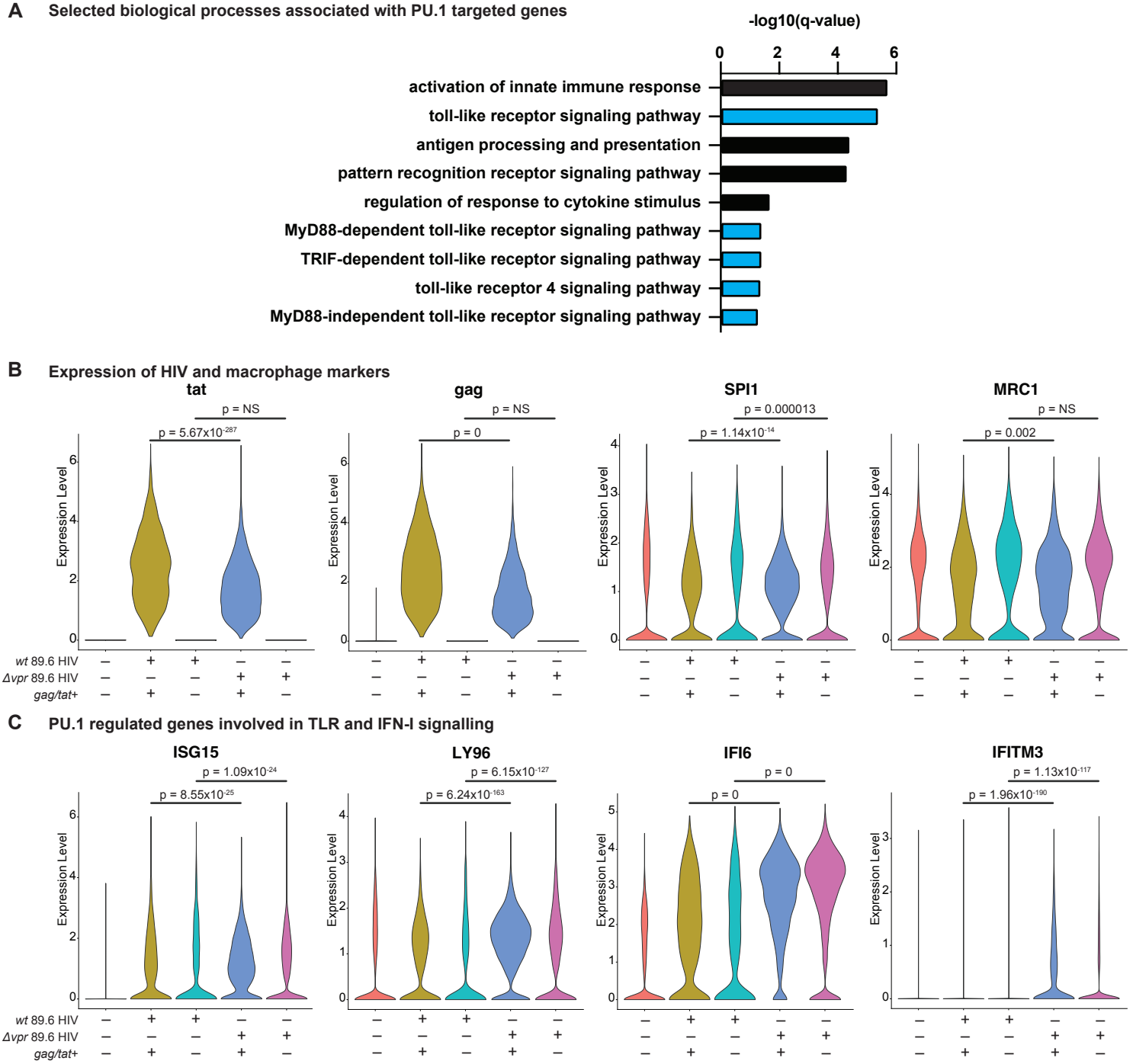

Figure 3. Vpr counteracts the innate immune response to HIV infection. (A) Selected biological processes associated with infection and inflammation (selected from GO terms represented in Figure 2D). Pathways were identified as associated with PU.1 regulated genes downmodulated in MDMs infected with 89.6^{wt} or $89.6^{\Delta vpr}$ virus as determined by expression of *gag* and *tat* transcripts (highlighted in Figure 2C). The -log10 FDR-adjusted p-values (q-values) are plotted for each gene ontology term. Blue bars represent terms associated with TLR signaling; Black bars represent related gene ontology terms similar, but not directly associated with TLR signaling. (B) Violin plots summarizing single-cell RNA transcripts expressed by primary human macrophages treated with the indicated virus and cultured for 10 days. *Gag+/tat+* are the subset of cells expressing HIV genes within in each culture. *SPI1* is the gene that codes for PU.1. *MRC1* is the gene that codes for mannose receptor. (C) Violin plots summarizing single-cell RNA transcripts expressed by primary human macrophages as in (B). False-discovery rate corrected Wilcoxon rank-sum p-values are shown above the conditions being compared.

203 replication-defective clone of HIV NL4-3 that expresses GFP in the *env* reading frame (Figure
204 4A). We transduced MDMs with this virus containing all intact accessory proteins, or with
205 additional mutations in the open reading frames of either *vpr, nef*, or both. PU.1 levels were
206 measured by flow cytometry at 5-, 7-, and 10-days post infection. Notably, we found that Vpr
207 expression resulted in lower PU.1 protein levels in infected (GFP^+) cells but not in virus-exposed
208 (GFP^-) bystander cells, whether Nef was expressed or not (Figure 4B, C). These changes in
209 PU.1 were consistently observed in MDMs from four independent donors (Figure 4C). Based on
210 these results, we concluded that Vpr downmodulates PU.1 in HIV-infected primary human
211 MDMs.
212
213 To determine whether Vpr was sufficient for PU.1 downmodulation, we tested the ability of
214 several 3xFLAG-tagged Vpr proteins derived from a panel of HIV molecular clones [89.6, NL4-3,
215 AD8 and YU2-Vpr (Figure 4D)] to reduce exogenous PU.1 expression in transfected HEK 293T
216 cells. Because the gene that encodes PU.1 (*SPI1*) contains PU.1 binding sites and is
217 downmodulated by Vpr expression (Figure 1B), for these experiments, PU.1 was expressed
218 under the control of a heterologous promoter that allowed separation of transcriptional and post-
219 transcriptional changes (Figure 4E). For comparison, we used the evolutionarily related protein,
220 Vpx, from the $HIV2_{ROD}$ molecular clone. We found that all Vpr-expression constructs tested
221 resulted in a notably lower level of PU.1 protein compared to PU.1 protein with HIV-2_{ROD}Vpx
222 (Figure 4F). Vpr-dependent reduced levels of PU.1 were consistently observed in four
223 independent experiments and were statistically significant (Figure 4G).
224
225 After determining that Vpr was sufficient to downmodulate PU.1 in HEK 293T cells, we
226 confirmed these results in a second cell line, the lymphoblastic chronic myelogenous leukemia
227 cell line K562, which endogenously expresses PU.1. For these experiments Vpr-expression was
228 achieved using VSV-G envelope pseudotyped lentiviruses. Like the results obtained in HEK
229 293T cells, infections with viruses expressing all Vprs tested (89.6, NL4-3, AD8, YU2) had lower
230 endogenous PU.1 levels compared to mock infection and HIV-2_{ROD}Vpx infection (Figure 4H).
231
232 Because the Vpr-dependent decrease of PU.1 occurred both for endogenous PU.1 expressed
233 from its native promoter in K562 cells as well as in HEK 293T cells, when PU.1 was expressed
234 from a heterologous promoter, we hypothesized that Vpr was affecting PU.1 protein levels post-
235 transcriptionally. To rule out transcriptional effects on the heterologous promoter, we quantified
236 PU.1 mRNA in HEK 293T cells transfected with a PU.1 expression plasmid and HIV constructs

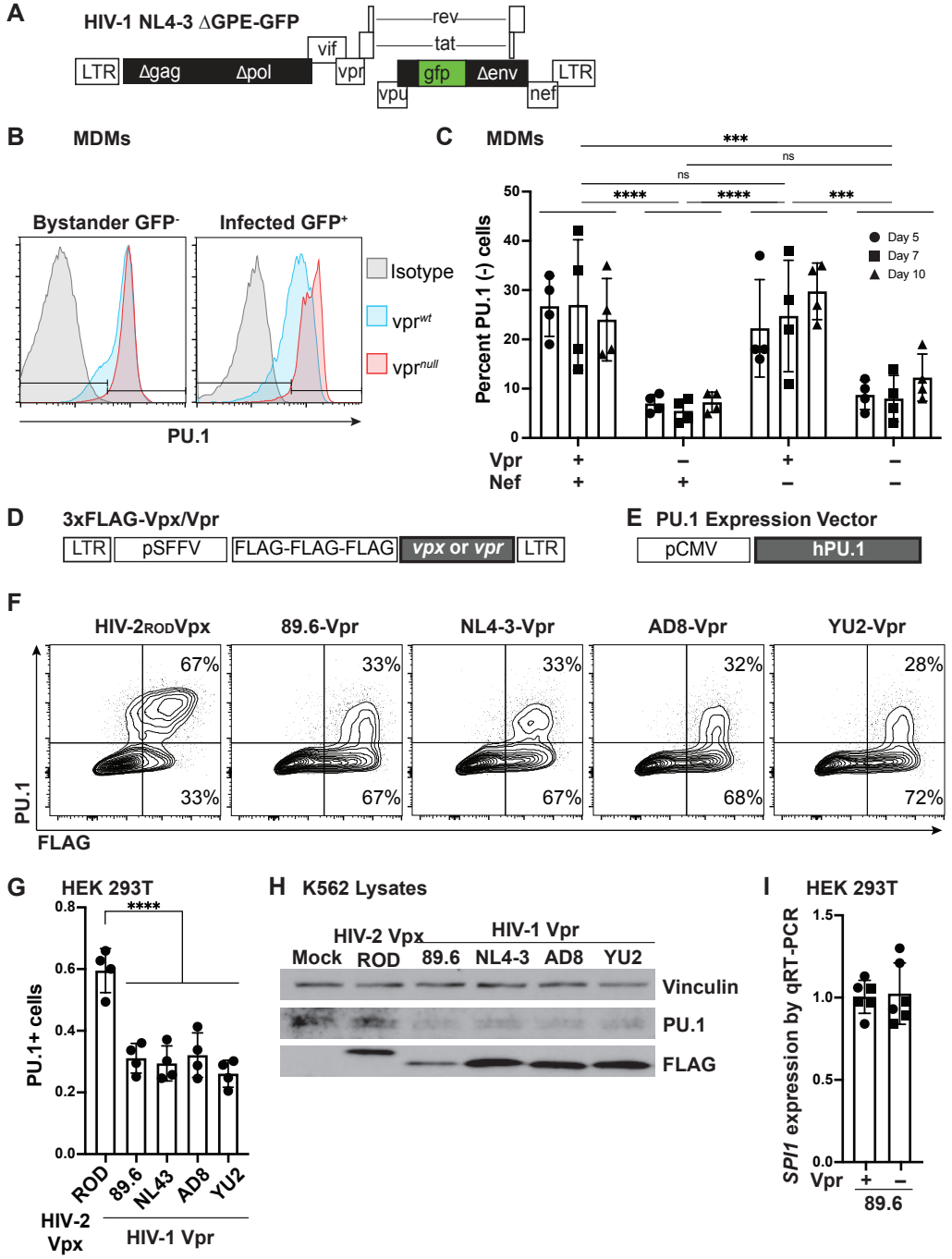

Figure 4. PU.1 levels decrease in the presence of Vpr. (A) NL4-3 ΔGPE-GFP viral genome map. (B) Representative flow cytometry histogram of PU.1 expression in infected (GFP$^+$) or uninfected bystander (GFP$^-$) MDMs infected with NL4-3 ΔGPE-GFP with or without *vpr* and collected on day 7 post infection. (C) Summary graph showing the percentage of infected (GFP$^+$) cells that do not express PU.1 as determined by flow cytometry as depicted in Figure 4B. The mean +/- standard deviation from n=4 independent donors is shown for each time point. P values were determined using an analysis of variance (ANOVA) with Tukey's multiple comparisons test. *** indicates p = 0.001, **** indicates p < 0.0001. (D) Lentiviral map of vectors encoding 3xFLAG-encoding *vpr* or *vpx* genes. (E) PU.1 expression plasmid map for full-length, human PU.1. (F) Representative flow cytometric plots of HEK 293T cells transiently transfected with PU.1 and the indicated FLAG-tagged viral protein. (G) Summary graph showing PU.1$^+$ expression in transfected (FLAG$^+$) cells. Each point represents the mean of three technical replicates. The mean +/- standard deviation of four independent experiments is shown. P values were determined using one-way ANOVA compared to control, **** indicates p < 0.0001. (H) Immunoblot analysis of PU.1 in K562 cells transduced with the indicated lentivirus expressing 3xFLAG-tagged viral proteins. Results are representative of those from three independent experiments. (I) Summary graph of *SPI1* (the gene encoding PU.1) expression in HEK 293T cells co-transfected with PU.1 and an 89.6 expression vector with or without an intact *vpr* open reading frame. *SPI1* levels were assessed from purified RNA using RT quantitative real time PCR. Results represent the mean fold change compared with wild type +/- standard deviation for samples performed in triplicate for two independent experiments.

237 derived from 89.6 that had or lacked the Vpr gene (Supplemental Figure 3A). As shown in
238 Figure 4I, Vpr did not reduce expression of PU.1 mRNA when expressed from a heterologous
239 promoter in transfected cells. Thus, we concluded that the mechanisms by which Vpr reduced
240 PU.1 protein in HEK 293T cells must be post-transcriptional. Moreover, in macrophages, Vpr
241 likely exerts negative effects directly on PU.1 protein and indirectly on PU.1 RNA through PU.1
242 binding sites in the *SPI1* promoter [50].
243
244 Prior reports indicated that PU.1 suppresses HIV gene expression in a Tat-reversible manner[51].
245 If true, Vpr-targeting of PU.1 could explain the upregulation of HIV genes observed in Vpr-
246 expressing HIV infected macrophages (Figure 1F). To attempt to confirm these results, we co-
247 transfected HEK 293T cells with a PU.1 expression plasmid (Figure 4E) and an 89.6-derived
248 HIV genome that expresses GFP constitutively and mCherry upon HIV activation, allowing us to
249 distinguish transfected cells through GFP expression and HIV-LTR activity through mCherry
250 expression (Supplemental Figure 3A). To eliminate any complications from Vpr-mediated
251 reduction of PU.1, we used an HIV genome that did not express *vpr*. Transfection of increasing
252 amounts of PU.1 plasmid with the same amount of HIV in all conditions, resulted in increasing
253 amounts of PU.1 protein as measured by flow cytometry (Supplemental Figure 3B, Left).
254 However, we failed to confirm a PU.1-dependent suppression of HIV-LTR activity (Supplemental
255 Figure 3B, Right).
256
257 **PU.1 downmodulation is a conserved activity of Vprs from HIV-2 and closely related SIV**
258 **molecular clones.** Vpr is highly conserved in lentiviruses, including HIV-2 and all SIV strains
259 [52,53]. Interestingly, HIV-2 and certain SIVs contain both Vpr and Vpx, whereas HIV-1 and some
260 SIVs contain only Vpr (Figure 5A). The extent to which these two proteins harbor overlapping
261 functions has been a subject of a number of research studies [17,54,55]. Thus, we first examined
262 whether Vprs from viruses containing both Vpr and Vpx would reduce PU.1 levels. To do this,
263 we used the HIV-2_{ROD} molecular clone from which our Vpx control is derived. Transient
264 transfection of HEK 293T cells with our PU.1 expression vector and either HIV-2_{ROD}Vpx, HIV-
265 2_{ROD}Vpr, or HIV-$1_{89.6}$Vpr confirmed a significant decrease in PU.1 for cells expressing Vpr^{ROD} or
266 $Vpr^{89.6}$ but not Vpx^{ROD} (Figure 5B, C). This indicates that Vpx and Vpr from the same molecular
267 clone have divergent functions with respect to PU.1 downmodulation.
268
269 We next tested the ability of Vpr from six isolates evolutionarily similar and disparate to HIV-1 to
270 determine whether the PU.1 targeting function of Vpr is evolutionarily conserved. Vpr

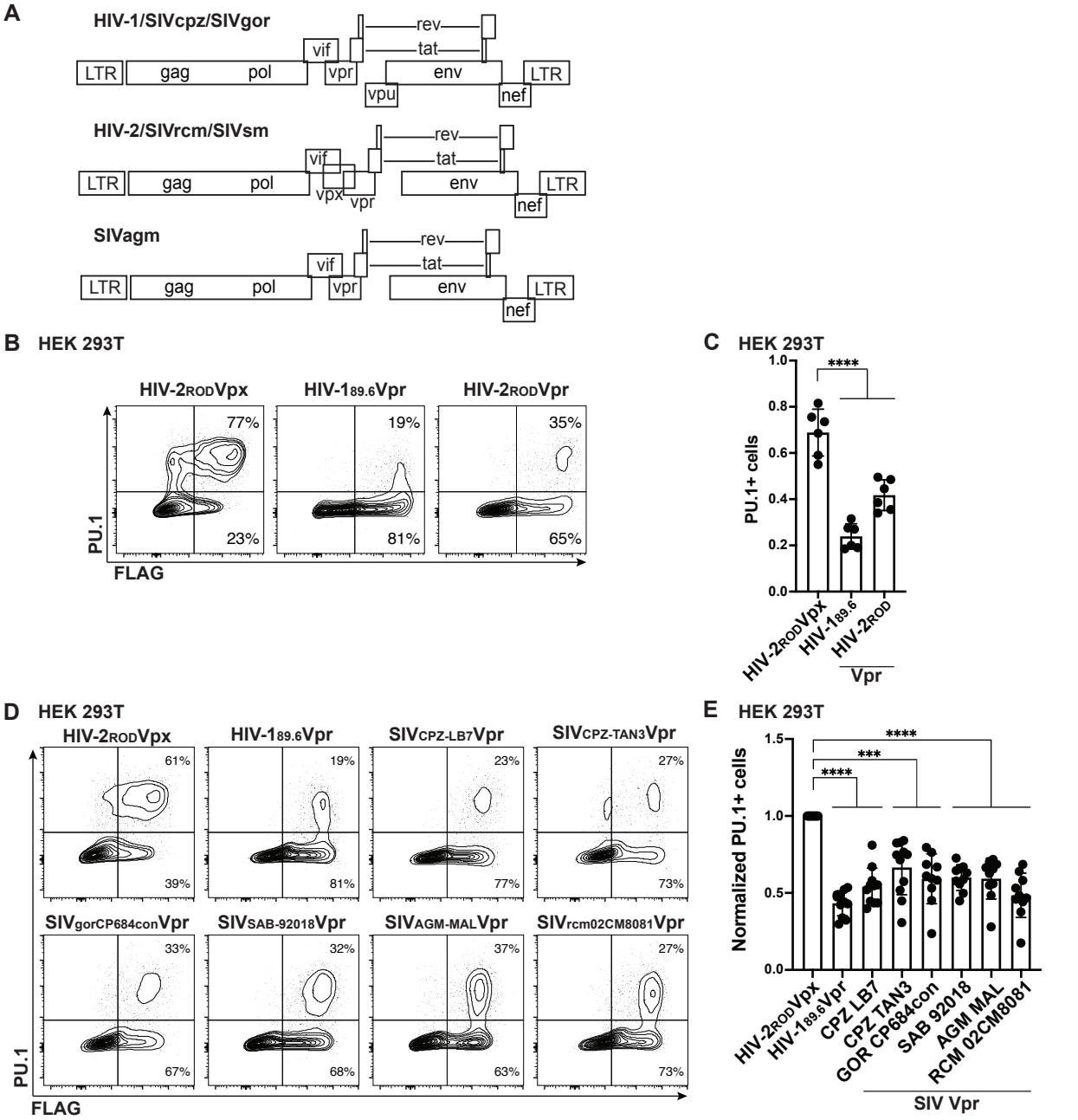

Figure 5. Vpr-mediated reduction of PU.1 is conserved in HIV-2 and SIV molecular clones. (A) Genomic maps for HIV-1, HIV-2, and select SIV genomes. HIV-1, SIVcpz, and SIVgor genomes contain *vpr* and *vpu* genes but not *vpx*. HIV-2, SIVrcm, and SIVsm contain *vpx* and *vpr*. SIVagm contains *vpr*. (B and D) Representative flow cytometric plots of HEK 293T cells transiently transfected with expression plasmids for PU.1 and the indicated FLAG-tagged viral protein. (C and E) Summary graph of data from B and D respectively. The percentage of PU.1$^+$ cells per transfected (FLAG$^+$) cells is shown. Each point represents the average of three technical replicates. The mean +/- standard deviation is shown for n=6 or 11 independent experiments, respectively. Part E was additionally normalized to HIV-2$_{ROD}$Vpx for each experiment. **** indicates $p < 0.0001$ using one-way ANOVA compared to control.

271 sequences from several SIV molecular clones from separate clades, including two from
272 chimpanzee and one from gorilla (the direct evolutionary relatives of HIV-1), were indeed able to
273 mediate the degradation of PU.1 in HEK 293T cells (Figures 5D, E). Thus, Vpr-mediated
274 reduction of PU.1 was consistently observed across all HIV-1, HIV-2, and SIV molecular clones
275 tested, indicating a strong selective pressure for HIV-related viruses to downmodulate PU.1 in
276 infected cells.
277
278 **Both PU.1 and DCAF1 form a complex with Vpr.** To determine whether Vpr recruits PU.1
279 similarly to other host proteins for proteasomal degradation via the CRL4-DCAF1 ubiquitin
280 ligase complex (Reviewed in [52]), we first assessed whether Vpr and PU.1 formed a complex in
281 transfected HEK 293T cells. Remarkably, we found that exogenously expressed PU.1 (Figure
282 4E) efficiently co-precipitated with FLAG-tagged 89.6-Vpr. In addition, and as expected [15,16],
283 DCAF1 also co-precipitated with Vpr (Figure 6A).
284
285 We next examined
286 whether Vpr co-
287 precipitated with
288 endogenous PU.1 in the
289 K562 cell line originally
290 derived from a patient
291 with CML[56]. To
292 accomplish this, we stably
293 expressed FLAG-tagged
294 HIV-$1_{89.6}$Vpr or HIV-
295 2_{ROD}Vpx in K562 cells
296 using lentiviral vectors
297 and repeated co-
298 immunoprecipitation
299 experiments. We found
300 that both PU.1 and

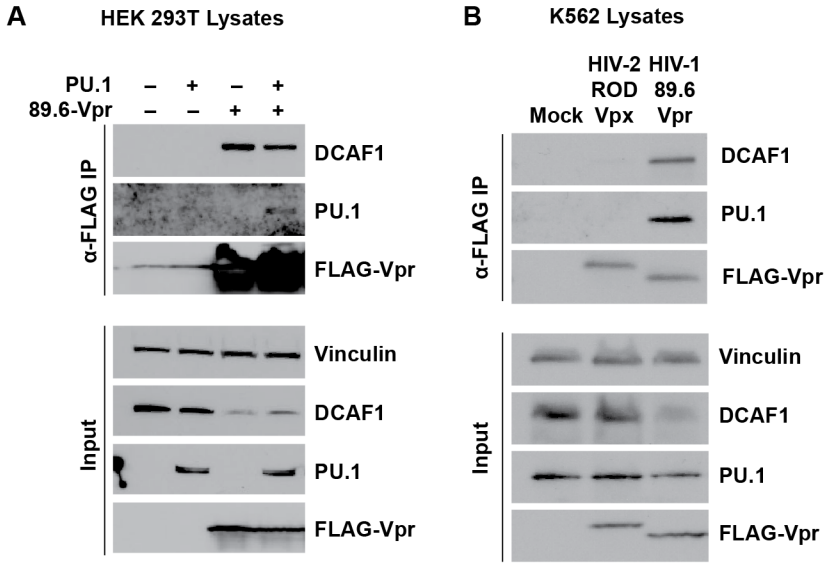

Figure 6. PU.1, and DCAF1 co-precipitate with Vpr but not Vpx. (A) Western blot analysis of lysates from HEK 293T cells co-transfected with the indicated expression constructs and immunoprecipitated with an antibody directed against the FLAG epitope. (B) Western blot analysis of lysates from K562 cells transduced with lentiviruses and treated as in part A. For parts A and B, results are representative of three independent experiments.

301 DCAF1 co-precipitated with Vpr to a greater extent than Vpx, again suggesting PU.1 binding is
302 specific to Vpr and not to the similar accessory protein Vpx (Figure 6B). Collectively, these data
303 indicate that Vpr selectively forms complexes with both PU.1 and DCAF1 in cells expressing
304 PU.1 at normal levels from an endogenous promoter.

305

306 **Interactions between PU.1 and Vpr require DCAF1**. To better understand the mechanism
307 through which Vpr downmodulates PU.1, we assessed a potential requirement for the host
308 protein DCAF1. DCAF1 (also known as VprBP[15]) is the Vpr binding partner in the CRL4
309 ubiquitin ligase complex, necessary for proteasomal degradation of Vpr recruited host proteins
310 (Refs). We generated an HEK 293T cell line with reduced DCAF1 expression. The cell line was
311 generated using a lentiviral vector stably expressing either a non-targeting shRNA (shScramble)
312 or a DCAF1-targeting shRNA cassette (shDCAF1) (Supplemental Figure 4; (Figure 7A, Lanes
313 1-6 compared to 7-12 and lanes 13-18 compared to 19-24, respectively).
314

315 Having previously demonstrated that PU.1 and DCAF1 co-precipitate with Vpr (Figure 6), we
316 performed the IP in reverse and found that Vpr and DCAF1 coprecipitated with a FLAG-tagged-
317 PU.1 (Figure 7A, Lanes 4 and 10). Because the antibody directed against Vpr does not
318 recognize 89.6-Vpr, these experiments utilizing un-tagged Vpr were performed using NL4-3,
319 whose Vpr is recognized by the antibody.
320

321 We found that the amount of Vpr that co-precipitated with PU.1 was decreased with DCAF1
322 silencing (Figure 7A, upper panel, Lane 10 compared to 4), suggesting a role for DCAF1 in the
323 interaction between Vpr and PU.1. Consistent with this, NL4-3-Vpr^{Q65R} protein, which is
324 defective for DCAF1 interactions[57,58], did not coprecipitate with PU.1 (Figure 7A, upper panel
325 Lanes 6 and 12 compared to 4 and 10). These interesting results suggest the unexpected
326 conclusion that PU.1, Vpr, and DCAF1 may form a trimeric complex and PU.1 binding in the
327 complex is dependent on both Vpr and DCAF1 (Figure 7D), though Vpr can associate with
328 DCAF1 independently of PU.1 (Figures 6A, B).
329

330 **Vpr downmodulates PU.1 via a pathway that depends on proteasome activity.**
331 To further test the relationship between PU.1 and the Vpr/DCAF1 complex, which together are
332 known to promote ubiquitylation and proteasomal degradation of Vpr-bound host proteins, we
333 investigated whether inhibition of the proteosome could restore PU.1 levels. As shown in Figure
334 7B, we were indeed able to restore PU.1 levels in transfected HEK 293T cells expressing Vpr
335 using MG132, as a specific inhibitor of the proteasome.
336

337 **An intact DCAF-1 interaction domain is required for Vpr and DCAF1 to co-precipitate with**
338 **TET2 and PU.1.** The PU.1-regulated antiviral factor, *IFITM3* (Figure 2C and E) is also controlled

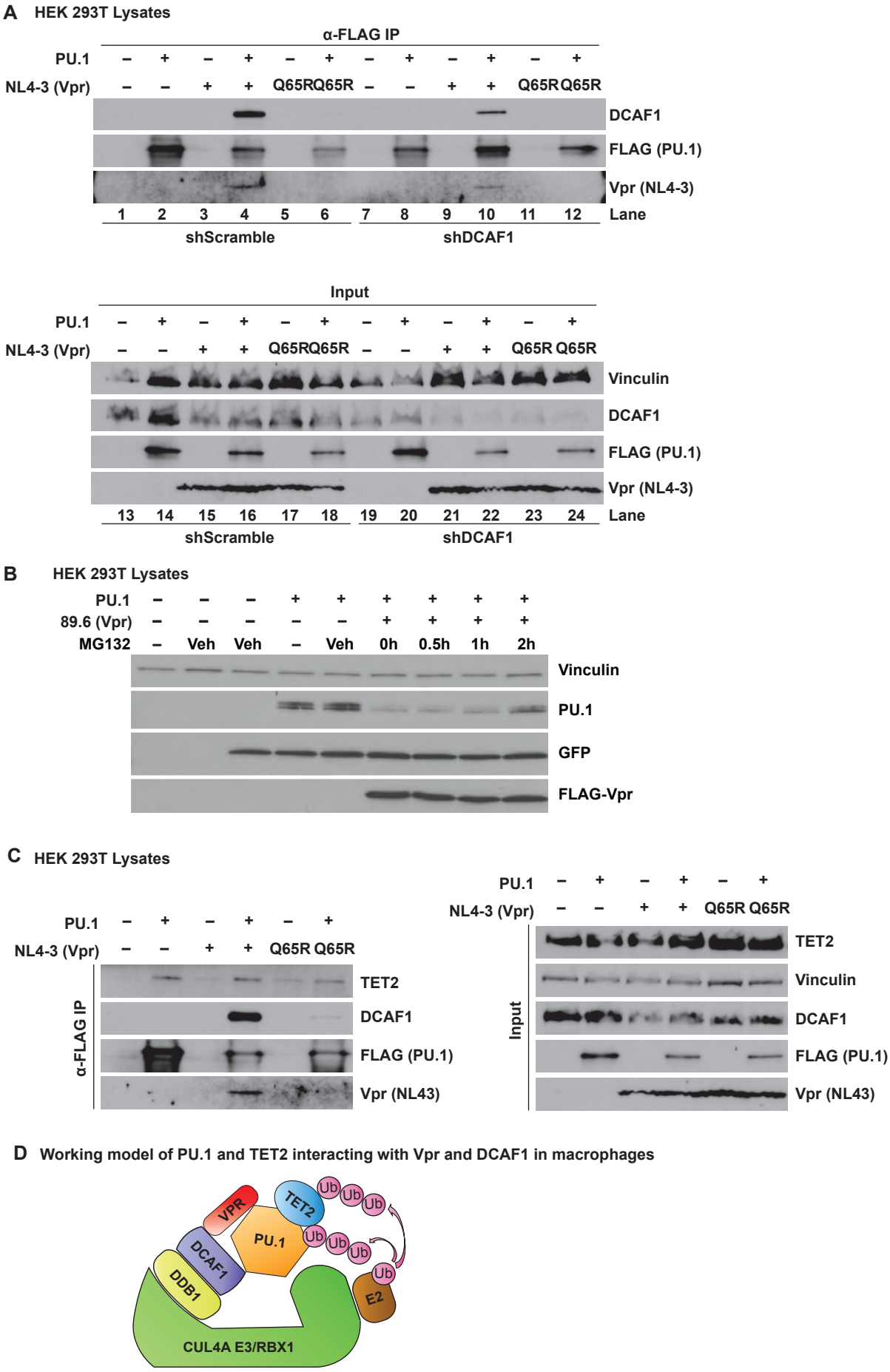

Figure 7. An intact DCAF-1 interaction domain is required for Vpr and DCAF1 to co-precipitate with TET2 and PU.1. (A) Western blot analysis of lysates from HEK 293T cells stably expressing either control, non-targeting shRNA (scramble) or an shRNA targeting DCAF1 (shDCAF1), transfected with the indicated expression plasmid and immunoprecipitated using an antibody directed against the FLAG epitope. (B) Western blot analysis of lysates from HEK 293T cells transfected with the indicated expression construct and treatment as indicated with 10μM MG132 or vehicle (Veh) control (DMSO). A GFP-expressing plasmid was included where indicated as control for transfection efficiency. (C) Western blot analysis of lysates from HEK 293T cells co-transfected with the indicated expression constructs and immunoprecipitated with an antibody directed against the FLAG epitope. For parts A, B, and C, results are representative of three independent experiments. (D) Working model of PU.1 and TET2 interacting with Vpr and DCAF1 in macrophages.

339 by TET2, another target of Vpr [36,37]. TET2 is a DNA dioxygenase that de-methylates the *IFITM3*
340 promoter during viral infection, inhibiting HIV Env trafficking and reducing viral spread[59,60]. To
341 prevent this, Vpr mediates the ubiquitination and degradation of TET2, which in turn inhibits
342 *IFITM3* expression. PU.1 also regulates myeloid specific gene expression by interacting with
343 other transcriptional regulatory proteins, including TET2[24,25,31]. We therefore hypothesized that
344 TET2 could be co-recruited with PU.1 to DCAF1 by Vpr for degradation (Figure 7D). Indeed, we
345 observed TET2 co-precipitating in HEK 293T cells with FLAG-tagged-PU.1, Vpr, and DCAF1
346 (Figure 7C). Our findings support a model in which Vpr can dramatically alter the transcriptional
347 landscape in macrophages by targeting myeloid-specific transcription factors – like PU.1 and its
348 co-factors – that are required for the expression of key antiviral restriction factors (Figure 8).

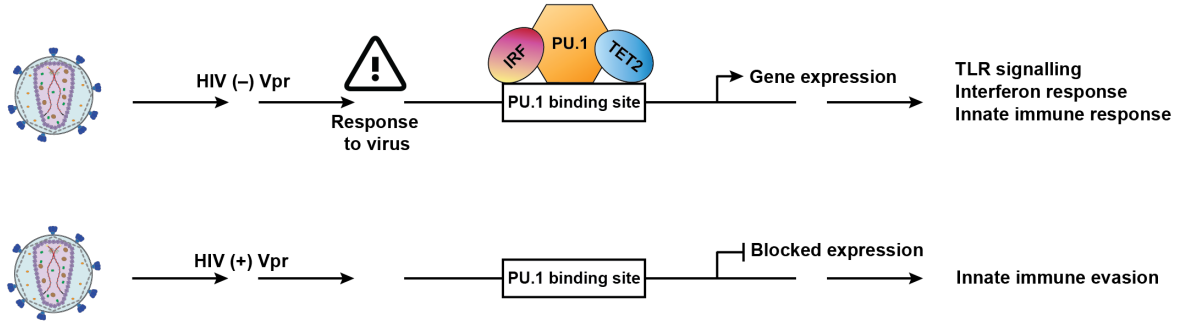

Figure 8. Proposed model of the PU.1-mediated antiviral response disrupted by HIV-Vpr. HIV (-) Vpr indicates an infection of primary macrophages with HIV that does not express Vpr. PU.1 protein is maintained and available to regulate anti-viral response genes with co-factors such as IRF or TET2. HIV (+) Vpr indicates an infection with HIV that expresses Vpr. PU.1 protein is less available to regulate anti-viral response genes, contributing to innate immune evasion.

349
350
351 **DISCUSSION**
352
353 Although HIV accessory proteins have been widely studied the critical function that drives
354 evolutionary conservation of Vpr has remained largely enigmatic. While Vpr significantly
355 enhances infection of macrophage-containing cultures, primarily by enhancing cell-to-cell
356 transmission, it does not substantially affect HIV infection in cultures of $CD4^+$ T cells that lack
357 macrophages [1–4,34,35,61]. While a number of Vpr targets implicated in post-replication DNA repair
358 have been identified, a compelling explanation for the dramatic selective effects of Vpr on
359 infection and spread in macrophage-containing cultures has remained elusive. In this work, we
360 identified a macrophage-specific target of Vpr, the myeloid transcription factor PU.1 and its
361 associated co-factors, which Vpr targets, averting antiviral effects (Figure 8). Remarkably, by
362 utilizing single-cell RNA sequencing of MDMs treated with replication competent virus with and
363 without Vpr we could distinguish effects of Vpr on cells harboring bona fide infections as well as

364 bystander cells. This allowed us to detect both cell autonomous and non-autonomous effects
365 of Vpr.
366
367 In infected cells, we found that Vpr reduces the transcription of hundreds of genes regulated
368 through PU.1 and its cofactors. Several of the PU.1 regulated genes we identified as being
369 impacted by Vpr are involved in TLR signaling. TLRs are highly conserved PRRs that help cells
370 identify PAMPs and respond quickly to infection. Activation of TLRs through binding of a PAMP,
371 initiates a cascade of intracellular signaling that results in the release of inflammatory cytokines
372 and upregulation of Type I interferon response genes[45,47,62]. The products of these genes have
373 known antiviral effects on in HIV, and include *ISG15*, *STMN1, IFI6, LY96*, *TREM2*, *FABP4*,
374 *IFITM3,* and *MRC1*. *STMN1* is thought to play a role in the establishment of HIV latency, and
375 depletion leads to higher expression of HIV-1[63]. *MRC1* and *IFITM3* interrupt Env trafficking,
376 reducing viral spread. *IFI6*, *LY96, and ISG15* are members of the Type I IFN response to
377 infection[46,64,65] and *ISG15* has also been shown to inhibit HIV spread by disrupting Gag
378 polymerization[66].
379
380 Unexpectedly, we found that bystander cells within HIV infected cultures also responded to HIV
381 infection by upregulating a subset of these antiviral genes, including *ISG15*, *LY96*, *IFI6*, and
382 *IFITM3.* Moreover, we found that upregulation of these factors was reduced in bystander cells
383 from Vpr-positive versus Vpr-negative HIV-infected primary macrophage cultures. By
384 comparison, other subsets of genes, including *SPI1* and *MRC1* were primarily
385 downmodulated in the infected subset and either not at all in the bystander cells or to a
386 lesser extent than their infected counterparts. Thus, we observed both cell autonomous and
387 non-autonomous effects of Vpr. Because we only detected significant downmodulation of PU.1
388 protein in the infected cell subset in our flow cytometric analyses (Figure 2B), Vpr does not
389 appear to enter and directly affect bystander cells in our cultures. Instead, the detrimental effect
390 of Vpr on antiviral gene expression in bystander cells likely occurs by an indirect mechanism.
391 We propose that the inhibitory effects of Vpr on PU.1/IRF gene regulation reduces the
392 expression of paracrine factors that alert bystander macrophages to the presence of the virus.
393 Likely candidate genes that could act in this way include type I interferons. Unfortunately, we
394 were unable to efficiently detect *IFN* RNA expression via single cell RNA sequencing.
395 Nevertheless, our results indicate that Vpr can exert systemic antiviral affects that favor virus
396 infection and spread.
397

398 We have previously shown that mannose receptor is a host restriction factor that reduces HIV
399 spread in macrophages by binding to mannose residues on Env and directing Env to the
400 lysosome for degradation[34]. However, our previous data lacked a mechanism for Vpr-mediated
401 transcriptional reduction of *MRC1* in macrophages. The data here confirm findings from other
402 groups that PU.1 regulates *MRC1* expression[42,51], and we provide new evidence that Vpr
403 reduces the transcriptional expression of *MRC1* in macrophages via PU.1 degradation.
404
405 In agreement with other studies[36,37], our unbiased survey of Vpr's effect on expression of host
406 transcriptome showed that Vpr reduced *IFITM3* gene expression substantially. IFITM proteins
407 are broad antiviral factors that inhibit viral entry and exit for HIV-1, SIV, MLV, VSV, EBOV,
408 WNV, among other viruses [67]. Of the IFITM proteins, IFITM3 is well documented as an HIV-1
409 antagonist. Like mannose receptor, IFITM3 interacts with Env in infected cells to inhibit Env
410 processing and virion incorporation and strongly inhibits cell-to-cell spread. Interruption of Env
411 processing by IFITM3 has been demonstrated for several HIV-1 molecular clones[68] many of
412 which were included within our own study (AD8, YU2, and NL4-3, HIV-2_{ROD}, SIVagm, and
413 SIVcpz). *IFITM3* expression is regulated by the DNA dioxygenase, TET2[36]. During HIV-1
414 infection of macrophages, in the absence of Vpr, TET2 demethylates the *IFITM3* promoter,
415 relieving suppression, contributing to the anti-viral response. When Vpr is present, *IFITM3*
416 expression is reduced after Vpr recruitment of TET2 to DCAF1 for polyubiquitination and
417 degradation of TET2[37]. Although TET2 is highly expressed in myeloid cells[69], it is ubiquitously
418 expressed in the nuclei of all cells[70]. How TET2 is specifically recruited to *IFITM3* to regulate
419 expression of *IFITM3* in macrophages remains unknown. Interestingly, in monocytes, TET2
420 interacts with PU.1, leading to interaction with genetic targets[31]. Therefore, we hypothesized
421 that Vpr exerts a macrophage-specific effect on the antiviral response by targeting PU.1 and by
422 extension, PU.1-associated proteins. Consistent with this hypothesis, we were able to
423 demonstrate TET2 immunoprecipitating with PU.1, Vpr, and DCAF1 (Figure 7). This provides
424 evidence that Vpr can re-program cellular transcription in macrophages by targeting myeloid-
425 specific transcription factors (Figure 1).
426
427 Vpr-mediated reduction of PU.1 occurred in all cell types tested in our study including MDM,
428 K562, and HEK 293T cells. The Vpr-dependent reduced PU.1 levels were observed regardless
429 of whether PU.1 was expressed from its native promoter or a heterologous promoter. Reversal
430 of PU.1 downmodulation with proteasome inhibitors in HEK 293T cells supports the conclusion
431 that Vpr directly reduces PU.1 protein by promoting its degradation. Vpr-mediated degradation

432 of PU.1 was consistent for all HIV-2, SIV, and HIV-1 Group M isolates tested - Group M being
433 largely responsible for the global HIV pandemic. In macrophages, *SPI1* mRNA levels encoding
434 PU.1 protein were also lower in the presence of Vpr, indicating that downmodulation of PU.1
435 can occur at both the transcriptional and the post-transcriptional level in macrophages.
436
437 It is important to note that we failed to confirm prior observations that PU.1 suppresses HIV-LTR
438 activity in a Tat reversible manner[51]. While it is possible that expression of Tat by our construct
439 prevented our ability to detect an effect of PU.1 on the HIV-1 LTR, these results nevertheless
440 indicate that downmodulation of PU.1 by Vpr is unlikely to impact HIV-1 gene expression in
441 infected macrophages that also express Tat. Thus, in primary HIV infected macrophages, Vpr
442 mainly targets PU.1 to counteract its anti-viral defense response rather than to counteract an
443 inhibitory effect on HIV gene expression. However, it is possible that the higher expression of
444 HIV genes we observed in Vpr-containing cells may result from Vpr counteracting a PU.1-
445 regulated factor that inhibits HIV gene transcription.
446
447 Vpr is highly conserved amongst primate lentiviruses and promotes infection of nondividing
448 cells, especially macrophages[61]. In addition, a requirement for Vpr to achieve maximal
449 replication and persistence in vivo was first discovered using an SIV molecular clone in rhesus
450 monkeys[71]. We therefore speculated that the ability of Vpr to degrade PU.1 is an important
451 evolutionary function of Vpr. HIV-2 differs from HIV-1 in that it contains Vpx, an accessory
452 protein that shares a common genetic ancestor with Vpr[53] but is lacking from all HIV-1
453 genomes. Thus, we tested the relative ability of Vpx and Vpr from the same molecular clone to
454 promote PU.1 degradation[53]. We were able to identify a unique function of HIV-2 Vpr to degrade
455 PU.1 that was not shared by Vpx. Similarly, both SIVcpz and SIVgor, the evolutionary
456 precursors to HIV-1, and Vpr proteins from more evolutionarily distant viruses were able to
457 consistently result in lower PU.1 levels. However, the greatest decrease in PU.1 levels was
458 achieved with HIV-1 derived molecular clones. We therefore speculate that the strength of Vpr-
459 mediated degradation of PU.1 plays an important role in driving spread in human pandemic
460 strains of HIV-1, and PU.1 may be a critical restriction factor, limiting spread between species
461 and within populations. However, more extensive studies comparing the relationship between
462 Vpr and PU.1 across SIV, HIV-2, and HIV-1 isolates is necessary and part of our ongoing
463 efforts.
464

465 The relationship between DCAF1 and Vpr is well documented[15–17]. We confirmed the binding of
466 Vpr to DCAF1 and identified PU.1 as a new Vpr-binding factor. We demonstrated that all three
467 components co-precipitate under many different cellular conditions regardless of whether we
468 pull-down with Vpr or PU.1. To our surprise, mutation of the glutamine residue at position 65 of
469 Vpr not only resulted in the loss of DCAF1 association but also disrupted formation of the Vpr-
470 PU.1 complex. Additionally, when we reduced DCAF1 levels, the amount of both Vpr and
471 DCAF1 precipitating with PU.1 was reduced. These results indicate that interactions amongst all
472 three proteins are necessary for stable complex formation, although further studies are
473 necessary to understand the detailed protein-protein interactions. Based on these findings, we
474 propose a model in which interactions amongst PU.1, Vpr, and DCAF1 promote the
475 ubiquitylation of PU.1 via the associated CUL4A ubiquitin ligase complex with resultant
476 proteasomal degradation (Figure 7D). Consistent with this model, inhibition of the proteosome
477 with MG132 treatment rescued PU.1 levels in the presence of Vpr.
478
479 Although the role of Vpr in HIV infection has remained largely undefined, we provide evidence
480 that the primary selective pressure for Vpr in lentiviruses is to disrupt the macrophage innate
481 antiviral response to infection, which is achieved by reducing PU.1 levels in infected cells. The
482 ability of Vpr to degrade PU.1 is highly conserved among all HIV-1, HIV-2, and SIV isolates
483 tested, and degradation of PU.1 relies on both Vpr and DCAF1. We are continuing to investigate
484 the transcriptional consequences of PU.1 degradation in macrophages. In addition to TET2,
485 PU.1 associates with other transcription factors in cells, potentially piggybacking other
486 secondary targets to the DCAF1-Cul4A E3 Ubiquitin ligase complex via Vpr. Because PU.1 is
487 necessary to maintain macrophage function, future studies should address the greater impact of
488 Vpr-mediated reduction of PU.1 on the infected macrophage.
489
490 **ACKNOWLEDGMENTS**
491 This work was supported by National Institutes of Health grants R01AI149669 to K.L.C. and
492 J.D.W., F31AI15504 to M.C.V. and F31AI125090-01 to J.L., R21AI32379 to K.L.C, training
493 grants T32GM007315 to M.C.V. and 5T32GM008353-27 to J.L., and additional funding provided
494 by the Rackham Regents Fellowship to M.C.V. We thank Chen Li from the Welch lab for his
495 invaluable advice and aid with single-cell data analysis. We thank the University of Michigan
496 Flow Cytometry Core and Advanced Genomics Core for assistance with experiments,
497 particularly Wenpu Trim and Tricia Tamsen. Thank you to all members of the Collins lab for their
498 helpful discussions.

AUTHOR CONTRIBUTIONS

Conceptualization, M.C.V, J.L., and K.L.C.; Methodology, M.C.V, J.L, J.D.W., and K.L.C.; Software, M.C.V. and J.D.W.; Validation, M.C.V.; Formal Analysis, M.C.V.; Investigation, M.C.V., W.M.D., T.C., and J.L.; Resources, K.L.C.; Writing – Original Draft, M.C.V.; Writing – Review & Editing, M.C.V., J.D.W., and K.L.C.; Visualization, M.C.V.; Supervision, J.D.W. and K.L.C., Funding Acquisition, M.C.V., J.D.W., and K.L.C.

DECLARATION OF INTEREST

The authors declare no competing interest.

509 **METHODS**

510

511 **Cell culture and preparation of human MDMs**

512 All cell cultures were maintained at 37°C in a 5% CO_2 humidified atmosphere. HEK 293Ts
513 (CRL-3216) and K562 (CCL-243) cells were obtained from ATCC and independently
514 authenticated by STR profiling. HEK 293Ts were maintained in DMEM medium (Gibco)
515 supplemented with 100 U/mL penicillin, 100µg/mL streptomycin, 2mM glutamine (Pen-Strep-
516 Glutamine, Invitrogen), and 10% fetal bovine serum (Invitrogen). K562 cell were maintained in
517 IMDM (Gibco) and supplemented as HEK293Ts. Monocyte-derived macrophages (MDMs) were
518 isolated and cultured as previously described[34] and maintained in R10 (RPMI, supplemented as
519 HEK 293Ts). Monocytes were isolated from anonymous donors by apheresis and obtained from
520 the New York Blood Center Component Laboratory. The use of human blood from anonymous,
521 de-identified donors was classified as non-human subject research in accordance with federal
522 regulations and therefore not subject to formal IRB review.

523

524 **Viruses, viral vectors, and expression plasmids**

525 The molecular clone p89.6 (cat# 3552 from Dr. Ronald G. Collman) was obtained from the AIDS
526 Reagent Program. The *vpr*-null version was generated as previously described[61]. The human,
527 full length PU.1 (hPU.1) expression vector was a gift of Dr. Gregory M. K. Poon and generated
528 as previously described[72]. A triple N-FLAG-tagged version of PU.1 was generated by using PCR
529 amplification of hPU.1 to add a KpnI site to the 5' end and EcoRI to the 3' end (5'
530 GTAGGTACCGCCACCATGGAAGGGTT primer and 3'
531 GTAGAATTCCACCACACTGGACTAGTG primer). The new product replaced an existing gene
532 when inserted into pcDNA3.1 containing a triple N-FLAG-tag between KpnI and EcoRI
533 (Addgene plasmid #67788). The GFP transfection control plasmid, pcDNA3-EGFP, was a gift
534 from Doug Golenbock (Addgene plasmid # 13031; http://n2t.net/addgene:13031; RRID:
535 Addgene_13031). The pNL4-3 ΔGPE-GFP plasmid used for single round infection of
536 macrophages was previously described[73], as were the vpr-null, nef-null, and vpr-nef null
537 versions[34]. pUC19[74] was used as control DNA to adjust transfection samples to the same final
538 DNA concentration. The p89.6-ΔGPEN-mCherry-pSFFV-EGFP single-round infection plasmid
539 was previously described[75] and further modified by replacing *gag* and *pol* with mCherry.
540 Deletion of *vpr* was achieved using Q5 Site-Directed Mutagenesis kit (New England Biolabs)
541 where the majority of the *vpr* coding sequence was deleted using PCR exclusion (forward -
542 CAGAATTGGGTGTCGACATAG, reverse - TCACAGCTTCATTCTTAAGC).

543

544 Triple FLAG-tagged Vpr and Vpx lentiviral expression vectors for HIV-2_{ROD}Vpx (Addgene
545 plasmid #115816), $SIV_{SAB-92018}$Vpr (Addgene plasmid #115822), $SIV_{AGM-MAL}$Vpr (Addgene
546 plasmid #115828), $SIV_{CPZ-TAN3}$Vpr (Addgene plasmid #115833), $SIV_{CPZ-LB7}$Vpr (Addgene plasmid
547 #115834), $SIV_{gorCP684con}$Vpr (Addgene plasmid #115835), and $SIV_{rcm02CM8081}$Vpr (Addgene
548 plasmid #115838) were a gift from Jeremy Luban[55]. Similar vectors for HIV-2_{ROD}Vpr, HIV-
549 $1_{89.6}$Vpr, HIV-1_{NL4-3}Vpr, HIV-1_{AD8}Vpr, HIV-1_{YU2}Vpr were generated by synthesizing the gene as a
550 gBlock (IDT, Coralville, Iowa, USA) between NotI and either EcoRI or AflIII in the same lentiviral
551 expression plasmid. Untagged expression vectors for HIV-1_{NL4-3}Vpr and HIV-$1_{NL4-3}$$Vpr^{Q65R}$ were
552 generated by synthesizing the genes as a gBlocks (IDT, Coralville, Iowa, USA) and inserting
553 them between SbfI and NotI in LeGO-IV, a gift from Boris Fehse (Addgene plasmid #27360)[76].
554

555 The short hairpin RNA targeting DCAF1 (target sequence: CCTCCCATTCTTCTGCCTTTA) was
556 designed using Genetic Perturbation Platform (Broad institute) and cloned into pLKO.1 – TRC
557 cloning vector, a gift from David Root (Addgene plasmid # 10878 ; http://n2t.net/addgene:10878
558 ; RRID:Addgene_10878)[77]. The control shRNA, scramble shRNA was a gift from David Sabatini
559 (Addgene plasmid # 1864 ; http://n2t.net/addgene:1864 ; RRID:Addgene_1864)[78].
560

561 **Co-transfections**

562 Co-transfections of 3xFLAG-Vpx/Vpr and hPU.1 were performed in HEK 293T cells. Cells were
563 plated at 1.6 x 10^5 per well in a 12-well dish. 24hrs after plating, 1ng of hPU.1, 500ng of
564 3xFLAG-Vpx/Vpr, and pUC19 to a total of 1µg of DNA per well were combined with 4µg of PEI,
565 mixed and added to each well. 48hrs later, cells were harvested for flow cytometry or
566 immunoblotting. For co-immunoprecipitations, transfection experiments were scaled to achieve
567 60 x 10^6 cells per condition. Co-transfections with p89.6-ΔGPERN-mCherry-pSFFV-EGFP and
568 hPU.1 were performed as described above and with DNA amounts described in the legend.
569

570 **Transduction of MDM, K562, and HEK 293T**

571 All transductions were performed via spin inoculation at 1050 x g for 2 hr at 25°C with equal
572 virus amounts determined by Gag p24 mass in medium containing 4µg/mL polybrene (Sigma).
573 MDMs were inoculated with 10µg p24 mass equivalents of NL4-3 ΔGPE-GFP virus. K562 and
574 HEK 293Ts were spin inoculated with 10µg p24 mass equivalents of shScramble and shDCAF1
575 viruses. K562 cells were inoculated with varying amounts of 3xFLAG-tagged Vpr/Vpx

576 expression viruses to achieve equal FLAG expression. After infection, viral medium was
577 removed and replaced with fresh medium.
578
579 **HIV infection of MDM**
580 Prior to infection, 500µL of medium was removed from each well of MDMs and saved to make
581 diluted conditioned media post-infection. MDM were infected with 5µg, 10µg, and 20µg
582 equivalents of Gag p24 mass in 500µL total of R10 6 hr at 37°C. After the 6 hr infection, media
583 was removed and replaced with conditioned media diluted 1:2 in R10. Half-media changes were
584 performed every three days.
585
586 **Single-cell RNA sequencing**
587 At 10 days post-infection, uninfected, 89.6^{WT}, and $89.6^{\Delta vpr}$ infected MDMs were lifted using
588 enzyme free cell dissociation buffer (ThermoFisher). Replicate samples were fixed with
589 paraformaldehyde and stained for Gag to assess viral spread by flow cytometry. The resulting
590 flow cytometry data was used to select 89.6^{WT} and $89.6^{\Delta vpr}$ conditions with similar percentages
591 of infected cells. Wells of the selected conditions were harvested, counted, and prepared
592 according to manufacturer instructions for 10X Chromium Next GEM Single Cell 3' v3 Gene
593 Expression (10X Genomics).
594
595 **Single-cell data analysis**
596 10X filtered expression matrices were generated from CellRanger version 3.0.0 (10X
597 Genomics). We analyzed all single-cell gene expression data using the standard LIGER[38]
598 (https://github.com/welch-lab/liger) data integration pipeline. All WT and Vpr-null infected MDM
599 raw data expression matrices from each donor were combined before merging the data. We
600 used a value of k = 20 during joint matrix factorization, of resolution of 0.05 for Louvain
601 clustering, and nearest neighbor = 30 with a minimum distance = 0.3 for UMAP visualization.
602 Infected cells were identified by sub-setting cells with a non-zero expression value for both *gag*
603 and *tat* transcripts. Differential gene expression between WT and Vpr-null infected MDMs was
604 determined using the Wilcoxin rank-sum test. Volcano plots of differentially expressed genes
605 was generated using ggplot2[79] (https://ggplot2.tidyverse.org/). Downregulated genes in the
606 presence of Vpr with a log2FC > 1 and adjusted p-value > 0.05 were used as input for the
607 HOMER[80] (http://homer.ucsd.edu/homer/motif/) 'findMotifs' function using the human reference
608 set. PU.1-motif associated genes were identified using the 'find' function in 'findMotifs' from
609 HOMER. Gene Ontology analysis for biological processes for PU.1 motif-containing genes was

610 determined using GOrilla[81,82] (http://cbl-gorilla.cs.technion.ac.il/) with PU.1 regulated genes as
611 target genes and all expressed genes in our dataset as background. Biological processes were
612 plotted using REVIGO[83] (http://revigo.irb.hr/). The -500bp sequence for MRC1 used for PU.1
613 motif scanning was obtained from UCSC Genome Browser[84] (https://genome.ucsc.edu/) using
614 Human reference genome GRCh38/hg38. The PU.1 binding motif probability matrix was
615 obtained from HOMER and used with FIMO[85] (https://meme-suite.org/meme/doc/fimo.html) to
616 scan the *MRC1* input sequence. Violin plots were generated by importing our LIGER generated
617 dataset into Seurat[86] (https://satijalab.org/seurat/) and running the VlnPlot function. All single-
618 cell data analysis and plots were done using RStudio[87] (http://www.rstudio.com/) except for
619 HOMER-predicted motifs.
620
621 **Virus production**
622 Virus stocks were produced by transfected HEK 293T cells (ATCC, Manassas, Virginia) with
623 viral DNA and polyethylenimine (PEI) as previously described[34]. For replication defective
624 constructs, cells were plated 24hrs before transfection with a DNA ratio of 1:1:1 with pCMV-HIV-
625 1[88], pHCMV-V (VSV-G expression plasmid) (ATCC 75497), and lentiviral expression plasmid.
626 Viral supernatant was collected two days post-transfection and stored at -80°C. For infectious
627 virus, pCMV-HIV and pHCMV-V were omitted.
628
629 **Virion quantification**
630 Viral supernatants were quantified by ELISA as previously described[34] with the following
631 modification: lysed samples were captured at 4℃ overnight.
632
633 **Immunoblot**
634 Western blots: cells were lysed in Blue Loading Buffer (cat# 7722, Cell Signaling Technology),
635 sonicated with a Misonix sonicator (Qsonica, LLC. Newtown, CT), boiled for 10min at 95°C
636 before loading, and analyzed by SDS-PAGE immunoblot.
637
638 Co-immunoprecipitation: cells were lysed in Pierce IP Lysis Buffer (Thermo Fisher Scientific)
639 and 1x Halt Protease Inhibitor Cocktail (Thermo Fisher Scientific). Lysates were incubated with
640 Anti-FLAG M2 Magnetic Beads (MilliporeSigma, Darmstadt, Germany) according to
641 manufacturer instructions. Proteins were eluted using 3xFLAG peptide (MilliporeSigma,
642 Darmstadt, Germany) and analyzed by SDS-PAGE immunoblot. FLAG-tagged proteins were
643 visualized using Pierce ECL (Thermo Scientific) after treatment with an HRP-conjugated primary

644 antibody directed against the FLAG epitope (Millipore Sigma). HRP-conjugated secondary
645 antibodies against murine and rabbit antibodies to other targets (see below) plus ECL Prime
646 reagent (Cytiva Amersham) were used to visualize all other proteins.
647
648 **Antibodies**
649 Antibodies to Vinculin (cat# V9131, Millipore Sigma), DCAF1 (cat# 11612-1AP, Proteintech),
650 PU.1 (cat# 2266S, Cell Signalling Technology), FLAG (cat# F1804, Millipore Sigma), TET2
651 (cat#MABE462, EMD Millipore), CAp24 (clone KC57-PE cat# 6604667, Beckman Coulter), Vpr
652 (AIDS Reagent Program cat# 3951 from Dr. Jeffrey Kopp), GFP (cat# ab13970, Abcam) were
653 used for immunoblot analysis. Secondary HRP conjugated antibodies against murine (rat anti-
654 mouse IgG1, eBioscience) and rabbit (goat anti-rabbit IgG, Invitrogen) were also used.
655 Antibodies to PU.1 (clone 7C6B05, BioLegend), FLAG (cat# 637324, BioLegend) were used for
656 flow cytometry.
657
658 **Quantitative RT PCR**
659 HEK 293T cells sorted as described in 'Flow Cytometry' below were counted using the
660 Countess II Cell Counter (Thermo Fisher Scientific) and cell samples were diluted such that all
661 conditions contained the same cell numbers as input. RNA was isolated using the Zymo
662 DirectZol RNA MiniPrep Plus extraction kit with an on-column DNaseI digestion. RNA was
663 reverse transcribed using the High-Capacity cDNA Reverse Transcriptase kit (Applied
664 Biosystems). Quantitative PCR was performed using SYBR green qPCR Master Mix (Applied
665 Biosystems) on a QuantStudio 3 Real-Time PCR System (Applied Biosystems) with
666 ReadyMade PrimeTime primers for *SPI1* (Integrated DNA Technologies Inc, USA) and RT2
667 qPCR Primer Assay for Human GAPDH (cat# PPH00150F-200, Qiagen). Expression was
668 quantified using ABI Sequence Detection software compared to serial dilutions of an SPI1 or
669 GAPDH synthetic sequence gBlock (Integrated DNA Technologies Inc, USA). Measured values
670 for *SPI1* were normalized to measured values of *GAPDH*.
671
672 **Flow cytometry**
673 For cells requiring intracellular staining using antibodies directed against HIV Gag p24, FLAG-
674 Vpx and -Vpr, and PU.1, paraformaldehyde-fixed cells were permeabilized with 0.1% Triton-X in
675 PBS for 2min followed by incubation with antibody for 30min at room temperature.
676 In all experiments, cells were gated sequentially by forward scatter vs. side scatter for cells and
677 then by forward scatter area vs. height to exclude doublets. All transduced MDMs and

678 transiently transfected HEK 293T cells were assessed for protein expression on the Cytek
679 Aurora. GFP+ HEK 293T cells in the MG132 treatment experiments and for qPCR were sorted
680 on the Sony SH800 cell sorter into R10. Untreated, GFP- cells were also sorted. All flow
681 cytometry data was analyzed using FlowJo software (TreeStar, Ashland, Oregon).
682
683 **Proteasome inhibition**
684 Lyophilized MG132 was purchased from MilliporeSigma (cat# M8699) and dissolved in DMSO.
685 MG132 was added to cellular medium to achieve a final concentration of 10μM at varying
686 timepoints. Cells were harvested from replicate wells such that all drug treatment timepoints
687 were collected at once. DMSO only control treatment wells (Vehicle) were treated with the same
688 volume of DMSO as contained in the MG132 treatment conditions.
689
690 **Statistical Analysis**
691 All non-single cell statistical analyses were performed using GraphPad Prism software as
692 described in figure legends for each experiment.

693 **FIGURE LEGENDS**

694

695 **Figure 1. Single-cell RNA sequencing of HIV-1 infected MDMs reveals Vpr-dependent**
696 **transcriptional changes.** (A) Schematic diagram illustrating the objective of single-cell RNA
697 sequencing; the identification of Vpr-targeted transcription factor(s) in HIV infected primary
698 macrophages. (B) Genome maps for full-length 89.6^{wt} HIV-1 (top) and the same viral genome
699 with a premature stop-codon in *vpr* (bottom). (C) Experimental setup for the generation of the
700 scRNA-seq datasets. (D) UMAP representation of LIGER-integrated scRNA-seq data from
701 MDM samples treated as shown in (C) and listed in Dataset. (E) UMAP representations of
702 LIGER-integrated scRNA-seq data from MDMs treated as indicated. (E, Right) Bona fide
703 infected cells were identified based on expression of HIV *tat* and *gag*. (E, left) Colors indicate
704 individual clusters. Cluster 0 = pro-inflammatory macrophages, Cluster 1 = cycling cells, Cluster
705 2 = dying cells, Cluster 3 = pro-inflammatory macrophages. (E, center and right) cells colored
706 according to whether they were exposed to 89.6 WT-Vpr virus (blue) or Vpr-null virus (pink). (F)
707 Volcano plot of differentially expressed genes from HIV 89.6^{wt} verses 89.6$^{\Delta vpr}$ infected MDMs
708 from (E) as determined by Wilcoxin Rank Sum. Significance determined as greater than 1 log2
709 fold change and false discovery rate adjusted p-value of $p < 0.05$ (red-bars). Blue colored genes
710 indicate genes less highly expressed in HIV 89.6^{wt} verses 89.6$^{\Delta vpr}$ infected MDMs, Red colored
711 genes indicate genes more highly expressed, and black colored genes indicate no significant
712 difference between datasets.

713

714 **Figure 2. Vpr downmodulates PU.1-dependent transcription.** (A) PU.1 motifs identified by
715 HOMER as present in the promoters of Vpr-downmodulated genes (Figure 1E, Blue). (B) Violin
716 plots displaying RNA abundance of the indicated transcription factor genes in MDMs infected
717 with the indicated virus. (C) Volcano plot as in Figure 1E except that genes containing a PU.1 or
718 PU.1-IRF binding motif in their promoter region are highlighted in green (See also Supplemental
719 Figure 2). (D) Biological processes associated with the PU.1 targeted genes from (B). Size of
720 circle indicates the relative number of GO terms with the process. FDR adjusted q-values
721 associated with GO terms as indicated by the color. (E) Violin plots displaying RNA abundance
722 of the indicated genes in MDMs infected with the indicated virus. HIV-1 89.6^{wt} (WT); HIV-1
723 89.6$^{\Delta vpr}$ (ΔVpr).

724

725 **Figure 3. Vpr counteracts the innate immune response to HIV infection.** (A) Selected
726 biological processes associated with infection and inflammation (selected from GO terms

727 represented in Figure 2D). Pathways were identified as associated with PU.1 regulated genes
728 downmodulated in MDMs infected with 89.6^{wt} or $89.6^{\Delta vpr}$ virus as determined by expression of
729 *gag* and *tat* transcripts (highlighted in Figure 2C). The -log10 FDR-adjusted p-values (q-values)
730 are plotted for each gene ontology term. Blue bars represent terms associated with TLR
731 signaling; Black bars represent related gene ontology terms similar, but not directly associated
732 with TLR signaling. (B) Violin plots summarizing single-cell RNA transcripts expressed by
733 primary human macrophages treated with the indicated virus and cultured for 10 days.
734 *Gag+/tat+* are the subset of cells expressing HIV genes within in each culture. *SPI1* is the gene
735 that codes for PU.1. *MRC1* is the gene that codes for mannose receptor. (C) Violin plots
736 summarizing single-cell RNA transcripts expressed by primary human macrophages as in (B).
737 False-discovery rate corrected Wilcoxon rank-sum p-values are shown above the conditions
738 being compared.
739
740 **Figure 4. PU.1 levels decrease in the presence of Vpr.** (A) NL4-3 ΔGPE-GFP viral genome
741 map. (B) Representative flow cytometry histogram of PU.1 expression in infected (GFP^+) or
742 uninfected bystander (GFP^-) MDMs infected with NL4-3 ΔGPE-GFP with or without *vpr* and
743 collected on day 7 post infection. (C) Summary graph showing the percentage of infected
744 (GFP^+) cells that do not express PU.1 as determined by flow cytometry as depicted in Figure
745 4B. The mean +/- standard deviation from n=4 independent donors is shown for each time point.
746 P values were determined using an analysis of variance (ANOVA) with Tukey's multiple
747 comparisons test. *** indicates $p = 0.001$, **** indicates $p < 0.0001$. (D) Lentiviral map of
748 vectors encoding 3xFLAG-encoding *vpr* or *vpx* genes. (E) PU.1 expression plasmid map for full-
749 length, human PU.1. (F) Representative flow cytometric plots of HEK 293T cells transiently
750 transfected with PU.1 and the indicated FLAG-tagged viral protein. (G) Summary graph showing
751 $PU.1^+$ expression in transfected ($FLAG^+$) cells. Each point represents the mean of three
752 technical replicates. The mean +/- standard deviation of four independent experiments is
753 shown. P values were determined using one-way ANOVA compared to control, **** indicates p
754 < 0.0001. (H) Immunoblot analysis of PU.1 in K562 cells transduced with the indicated lentivirus
755 expressing 3xFLAG-tagged viral proteins. Results are representative of those from three
756 independent experiments. (I) Summary graph of *SPI1* (the gene encoding PU.1) expression in
757 HEK 293T cells co-transfected with PU.1 and an 89.6 expression vector with or without an intact
758 *vpr* open reading frame. *SPI1* levels were assessed from purified RNA using RT quantitative
759 real time PCR. Results represent the mean fold change compared with wild type +/- standard
760 deviation for samples performed in triplicate for two independent experiments.

761

762 **Figure 5. Vpr-mediated reduction of PU.1 is conserved in HIV-2 and SIV molecular clones.**
763 (A) Genomic maps for HIV-1, HIV-2, and select SIV genomes. HIV-1, SIVcpz, and SIVgor
764 genomes contain *vpr* and *vpu* genes but not *vpx*. HIV-2, SIVrcm, and SIVsm contain *vpx* and
765 *vpr*. SIVagm contains *vpr*. (B and D) Representative flow cytometric plots of HEK 293T cells
766 transiently transfected with expression plasmids for PU.1 and the indicated FLAG-tagged viral
767 protein. (C and E) Summary graph of data from B and D respectively. The percentage of $PU.1^+$
768 cells per transfected ($FLAG^+$) cells is shown. Each point represents the average of three
769 technical replicates. The mean +/- standard deviation is shown for n=6 or 11 independent
770 experiments, respectively. Part E was additionally normalized to HIV-2_{ROD}Vpx for each
771 experiment. **** indicates $p < 0.0001$ using one-way ANOVA compared to control.
772

773 **Figure 6. PU.1, and DCAF1 co-precipitate with Vpr but not Vpx**. (A) Western blot analysis of
774 lysates from HEK 293 T cells co-transfected with the indicated expression constructs and
775 immunoprecipitated with an antibody directed against the FLAG epitope. (B) Western blot
776 analysis of lysates from K562 cells transduced with lentiviruses and treated as in part A. For
777 parts A and B, results are representative of three independent experiments.
778

779 **Figure 7. An intact DCAF-1 interaction domain is required for Vpr and DCAF1 to co-**
780 **precipitate with TET2 and PU.1.** (A) Western blot analysis of lysates from HEK 293T cells
781 stably expressing either control, non-targeting shRNA (scramble) or an shRNA targeting DCAF1
782 (shDCAF1), transfected with the indicated expression plasmid and immunoprecipitated using an
783 antibody directed against the FLAG epitope. (B) Western blot analysis of lysates from HEK
784 293T cells transfected with the indicated expression construct and treatment as indicated with
785 10μM MG132 or vehicle (Veh) control (DMSO). A GFP-expressing plasmid was included where
786 indicated as control for transfection efficiency. (C) Western blot analysis of lysates from HEK
787 293T cells co-transfected with the indicated expression constructs and immunoprecipitated with
788 an antibody directed against the FLAG epitope. For parts A, B, and C, results are representative
789 of three independent experiments. (D) Working model of PU.1 and TET2 interacting with Vpr
790 and DCAF1 in macrophages.
791

792 **Figure 8. Proposed model of the PU.1-mediated antiviral response disrupted by HIV-Vpr.**
793 HIV (-) Vpr indicates an infection of primary macrophages with HIV that does not express Vpr.
794 PU.1 protein is maintained and available to regulate anti-viral response genes with co-factors

795 such as IRF or TET2. HIV (+) Vpr indicates an infection with HIV that expresses Vpr. PU.1
796 protein is less available to regulate anti-viral response genes, contributing to innate immune
797 evasion.
798
799 **Supplemental Figure legends**
800
801 **Supplemental Table 1. MDM infection rates measured with Gag.** Percent infection of 89.6^{wt}
802 and $89.6^{\Delta vpr}$ infected MDMs from each of three donors was determined by quantifying the
803 percent Gag^{+} cells by either flow cytometry (protein) or gene expression levels from scRNA-seq
804 data (mRNA), as indicated by the experiment type and molecule, over the total number of cells
805 analyzed.
806
807 **Supplemental Figure 1. Transcription factors and their predicted binding motifs in**
808 **downregulated genes in MDMs expressing Vpr.** Motifs, transcription factor names,
809 significance (FDR q-value), and number of target genes identified by HOMER analysis of genes
810 downregulated in the presence of Vpr (Figure 1E) from several transcription factor families.
811
812 **Supplemental Figure 2. The *MRC1* promoter contains multiple PU.1 binding motifs.** The
813 first 500 bp upstream of the start codon in *MRC1*, the gene that codes for mannose receptor.
814 Previously reported PU.1 binding motifs are outlined in red. The double-box PU.1 motif was
815 identified through inputting the HOMER generated PU.1 motif parameters into FIMO (Find
816 Individual Motif Occurrences). The TATA box is outlined in blue, the 5'UTR in yellow, and the
817 start codon in green.
818
819 **Supplemental Figure 3. PU.1 does not alter HIV-LTR activity.** (A) Genomic map for 89.6-
820 derived HIV-1 fluorescent reporter virus (89.6-ΔGPERN-pSFFV-EGFP). (B) Representative flow
821 plots and bar graph assessing transfection rate via GFP expression in HEK 293T cells
822 transfected with the indicated amount of PU.1 construct from Figure 2E plus 500ng of 89.6-
823 ΔGPERN-pSFFV-EGFP from (A). (C) Summary graph of PU.1 expression in GFP^{+} cells from
824 (B). PU.1 levels were assessed using intracellular staining as described in Methods and
825 measured by flow cytometry. (D) Summary graph of HIV-LTR activity as assessed by mCherry
826 MFI from the same cells as in (C), measured flow cytometrically. All conditions were transfected
827 with 500ng of HIV expression plasmid plus 0, 1, 10, 100, or 500ng of PU.1 plasmid. MFI = mean
828 fluorescence intensity.

829

830 **Supplemental Figure 4. DCAF1 protein is reduced in K562 cells via shRNA.** Immunoblot of
831 lysates from K562 cells stably transduced with virus expressing a non-targeting shRNA
832 (shScramble) or one targeting DCAF1 (shDCAF1) compared to un-transduced cells (Mock).

833 **REFERENCES**

834

835 1. Balliet, J. W. *et al.* Distinct Effects in Primary Macrophages and Lymphocytes of the Human
836 Immunodeficiency Virus Type 1 Accessory Genes vpr, vpu, and nef: Mutational Analysis of a
837 Primary HIV-1 Isolate. *Virology* **200**, 623–631 (1994).
838 2. Eckstein, D. A. *et al.* HIV-1 Vpr enhances viral burden by facilitating infection of tissue
839 macrophages but not nondividing CD4+ T cells. *J. Exp. Med.* **194**, 1407–1419 (2001).
840 3. Connor, R. I., Chen, B. K., Choe, S. & Landau, N. R. Vpr Is Required for Efficient Replication of
841 Human Immunodeficiency Virus Type-1 in Mononuclear Phagocytes. *Virology* **206**, 935–944
842 (1995).
843 4. Dedera, D., Hu, W., Vander Heyden, N. & Ratner, L. Viral protein R of human
844 immunodeficiency virus types 1 and 2 is dispensable for replication and cytopathogenicity
845 in lymphoid cells. *J. Virol.* **63**, 3205–3208 (1989).
846 5. Rücker, E., Grivel, J.-C., Münch, J., Kirchhoff, F. & Margolis, L. Vpr and Vpu Are Important for
847 Efficient Human Immunodeficiency Virus Type 1 Replication and CD4+ T-Cell Depletion in
848 Human Lymphoid Tissue Ex Vivo. *J. Virol.* **78**, 12689–12693 (2004).
849 6. Lu, Y. L., Spearman, P. & Ratner, L. Human immunodeficiency virus type 1 viral protein R
850 localization in infected cells and virions. *J. Virol.* **67**, 6542–6550 (1993).
851 7. Laguette, N. *et al.* Premature Activation of the SLX4 Complex by Vpr Promotes G2/M Arrest
852 and Escape from Innate Immune Sensing. *Cell* **156**, 134–145 (2014).
853 8. Yan, J., Shun, M. C., Zhang, Y., Hao, C. & Skowronski, J. HIV-1 Vpr counteracts HLTF-
854 mediated restriction of HIV-1 infection in T cells. *Proc. Natl. Acad. Sci. U. S. A.* **116**, 9568–
855 9577 (2019).
856 9. Ahn, J. *et al.* HIV-1 Vpr Loads Uracil DNA Glycosylase-2 onto DCAF1, a Substrate Recognition
857 Subunit of a Cullin 4A-RING E3 Ubiquitin Ligase for Proteasome-dependent Degradation *. *J.*
858 *Biol. Chem.* **285**, 37333–37341 (2010).
859 10. Lahouassa, H. *et al.* HIV-1 Vpr degrades the HLTF DNA translocase in T cells and
860 macrophages. *Proc. Natl. Acad. Sci.* **113**, 5311–5316 (2016).

861 11. Withers-Ward, E. S., Mueller, T. D., Chen, I. S. Y. & Feigon, J. Biochemical and Structural
862 Analysis of the Interaction between the UBA(2) Domain of the DNA Repair Protein HHR23A
863 and HIV-1 Vpr. *Biochemistry* **39**, 14103–14112 (2000).
864 12. Wang, X. *et al.* HIV-1 Vpr Protein Inhibits Telomerase Activity via the EDD-DDB1-VPRBP E3
865 Ligase Complex *. *J. Biol. Chem.* **288**, 15474–15480 (2013).
866 13. Romani, B., Baygloo, N. S., Aghasadeghi, M. R. & Allahbakhshi, E. HIV-1 Vpr Protein
867 Enhances Proteasomal Degradation of MCM10 DNA Replication Factor through the Cul4-
868 DDB1[VprBP] E3 Ubiquitin Ligase to Induce G2/M Cell Cycle Arrest *. *J. Biol. Chem.* **290**,
869 17380–17389 (2015).
870 14. Yan, J. *et al.* HIV-1 Vpr Reprograms CLR4DCAF1 E3 Ubiquitin Ligase to Antagonize
871 Exonuclease 1-Mediated Restriction of HIV-1 Infection. *mBio* **9**, e01732-18 (2018).
872 15. Zhang, S., Feng, Y., Narayan, O. & Zhao, L.-J. Cytoplasmic retention of HIV-1 regulatory
873 protein Vpr by protein-protein interaction with a novel human cytoplasmic protein VprBP.
874 *Gene* **263**, 131–140 (2001).
875 16. McCall, C. M. *et al.* Human Immunodeficiency Virus Type 1 Vpr-Binding Protein VprBP, a
876 WD40 Protein Associated with the DDB1-CUL4 E3 Ubiquitin Ligase, Is Essential for DNA
877 Replication and Embryonic Development. *Mol. Cell. Biol.* **28**, 5621–5633 (2008).
878 17. Romani, B. & Cohen, É. A. Lentivirus Vpr and Vpx accessory proteins usurp the cullin4–DDB1
879 (DCAF1) E3 ubiquitin ligase. *Curr. Opin. Virol.* **2**, 755–763 (2012).
880 18. Hakata, Y., Miyazawa, M. & Landau, N. R. Interactions with DCAF1 and DDB1 in the CRL4 E3
881 ubiquitin ligase are required for Vpr-mediated G2 arrest. *Virol. J.* **11**, 108 (2014).
882 19. Schröfelbauer, B., Hakata, Y. & Landau, N. R. HIV-1 Vpr function is mediated by interaction
883 with the damage-specific DNA-binding protein DDB1. *Proc. Natl. Acad. Sci. U. S. A.* **104**,
884 4130–4135 (2007).
885 20. Belzile, J.-P. *et al.* HIV-1 Vpr-Mediated G2 Arrest Involves the DDB1-CUL4AVPRBP E3
886 Ubiquitin Ligase. *PLoS Pathog.* **3**, e85 (2007).
887 21. Hrecka, K. *et al.* HIV-1 and HIV-2 exhibit divergent interactions with HLTF and UNG2 DNA
888 repair proteins. *Proc. Natl. Acad. Sci. U. S. A.* **113**, E3921–E3930 (2016).

889 22. Lavin, Y., Mortha, A., Rahman, A. & Merad, M. Regulation of macrophage development and
890 function in peripheral tissues. *Nat. Rev. Immunol.* **15**, 731–744 (2015).
891 23. Silvin, A. & Manel, N. Innate immune sensing of HIV infection. *Curr. Opin. Immunol.* **32**, 54–
892 60 (2015).
893 24. Turkistany, S. A., Dekoter, R. P. & Hirszfeld, Ó. L. The Transcription Factor PU.1 is a Critical
894 Regulator of Cellular Communication in the Immune System. doi:10.1007/s00005-011-
895 0147-9.
896 25. Fisher, R. C. & Scott, E. W. Role of PU.1 in Hematopoiesis. *Stem Cells* **16**, 25–37 (1998).
897 26. Dakic, A. *et al.* PU.1 regulates the commitment of adult hematopoietic progenitors and
898 restricts granulopoiesis. *J. Exp. Med.* **201**, 1487–1502 (2005).
899 27. Gupta, P., Gurudutta, G. U., Saluja, D. & Tripathi, R. P. PU.1 and partners: regulation of
900 haematopoietic stem cell fate in normal and malignant haematopoiesis. *J. Cell. Mol. Med.*
901 **13**, 4349–4363 (2009).
902 28. Graves, B. J. & Petersen, J. M. Specificity within the ets Family of Transcription Factors. in
903 *Advances in Cancer Research* (eds. Vande Woude, G. F. & Klein, G.) vol. 75 1–57 (Academic
904 Press, 1998).
905 29. Marecki, S. & Fenton, M. J. PU.1/interferon regulatory factor interactions. *Cell Biochem.*
906 *Biophys.* **33**, 127–148 (2000).
907 30. Imperato, M. R., Cauchy, P., Obier, N. & Bonifer, C. The RUNX1–PU.1 axis in the control of
908 hematopoiesis. *Int. J. Hematol.* **101**, 319–329 (2015).
909 31. de la Rica, L. *et al.* PU.1 target genes undergo Tet2-coupled demethylation and DNMT3b-
910 mediated methylation in monocyte-to-osteoclast differentiation. *Genome Biol.* **14**, 1–21
911 (2013).
912 32. Liang, G. *et al.* Membrane metalloprotease TRABD2A restricts HIV-1 progeny production in
913 resting CD4 + T cells by degrading viral Gag polyprotein. *Nat. Immunol.* (2019)
914 doi:10.1038/s41590-019-0385-2.
915 33. Linehan, S. A., Martínez-Pomares, L., Stahl, P. D. & Gordon, S. Mannose Receptor and Its
916 Putative Ligands in Normal Murine Lymphoid and Nonlymphoid Organs: In Situ Expression

917 of Mannose Receptor by Selected Macrophages, Endothelial Cells, Perivascular Microglia,
918 and Mesangial Cells, but not Dendritic Cells. *J. Exp. Med.* **189**, 1961–1972 (1999).
919 34. Lubow, J. *et al.* Mannose receptor is an HIV restriction factor counteracted by Vpr in
920 macrophages. *eLife* **9**, (2020).
921 35. Collins, D. R., Lubow, J., Lukic, Z., Mashiba, M. & Collins, K. L. Vpr Promotes Macrophage-
922 Dependent HIV-1 Infection of CD4+ T Lymphocytes. *PLoS Pathog.* **11**, e1005054 (2015).
923 36. Wang, Q. & Su, L. Vpr Enhances HIV-1 Env Processing and Virion Infectivity in Macrophages
924 by Modulating TET2-Dependent IFITM3 Expression. *mBio* **10**, e01344-19 (2019).
925 37. Lv, L. *et al.* Vpr Targets TET2 for Degradation by CRL4VprBP E3 Ligase to Sustain IL-6
926 Expression and Enhance HIV-1 Replication. *Mol. Cell* **70**, 961-970.e5 (2018).
927 38. Welch, J. D. *et al.* Single-Cell Multi-omic Integration Compares and Contrasts Features of
928 Brain Cell Identity. *Cell* **177**, 1873–1887 (2019).
929 39. Zhang, F. & Bieniasz, P. D. HIV-1 Vpr induces cell cycle arrest and enhances viral gene
930 expression by depleting CCDC137. *eLife* **9**, e55806 (2020).
931 40. Pham, T. H. *et al.* Mechanisms of in vivo binding site selection of the hematopoietic master
932 transcription factor PU.1. *Nucleic Acids Res.* **41**, 6391–6402 (2013).
933 41. Buckland, J. Haematopoiesis: PU.1 pinned down. *Nat. Rev. Immunol.* **2**, 149 (2002).
934 42. Caldwell, R. L., Egan, B. S. & Shepherd, V. L. HIV-1 Tat Represses Transcription from the
935 Mannose Receptor Promoter. *J. Immunol.* **165**, 7035–7041 (2000).
936 43. Medzhitov, R., Preston-Hurlburt, P. & Janeway, C. A. A human homologue of the Drosophila
937 Toll protein signals activation of adaptive immunity. *Nature* **388**, 394–397 (1997).
938 44. Molteni, M., Gemma, S. & Rossetti, C. The Role of Toll-Like Receptor 4 in Infectious and
939 Noninfectious Inflammation. *Mediators Inflamm.* **2016**, 6978936 (2016).
940 45. Beutler, B. A. TLRs and innate immunity. *Blood* **113**, 1399–1407 (2009).
941 46. Perng, Y. C. & Lenschow, D. J. ISG15 in antiviral immunity and beyond. *Nat. Rev. Microbiol.*
942 **16**, 423–439 (2018).
943 47. Schneider, W. M., Chevillotte, M. D. & Rice, C. M. Interferon-Stimulated Genes: A Complex
944 Web of Host Defenses. *Annu. Rev. Immunol.* **32**, 513–545 (2014).

945 48. Shimazu, R. *et al.* MD-2, a Molecule that Confers Lipopolysaccharide Responsiveness on
946 Toll-like Receptor 4. *J. Exp. Med.* **189**, 1777–1782 (1999).
947 49. Nagai, Y. *et al.* Essential role of MD-2 in LPS responsiveness and TLR4 distribution. *Nat.*
948 *Immunol.* **3**, 667–672 (2002).
949 50. Chen, H. *et al.* PU.1 (Spi-1) autoregulates its expression in myeloid cells. *Oncogene* **11**,
950 1549–1560 (1995).
951 51. Kao, S. *et al.* The Myeloid-Specific Transcription Factor PU.1 Upregulates Mannose Receptor
952 Expression but Represses Basal Activity of the HIV-LTR Promoter. *J. Virol.* **96**, e00652-22
953 (2022).
954 52. Collins, D. R. & Collins, K. L. HIV-1 accessory proteins adapt cellular adaptors to facilitate
955 immune evasion. *PLoS Pathog.* **10**, e1003851 (2014).
956 53. Sharp, P. M. & Hahn, B. H. Origins of HIV and the AIDS Pandemic. *Cold Spring Harb.*
957 *Perspect. Med.* **1**, a006841 (2011).
958 54. Sakai, Y. *et al.* Expression Profiles of Vpx/Vpr Proteins Are Co-related with the Primate
959 Lentiviral Lineage. *Front. Microbiol.* **7**, (2016).
960 55. Yurkovetskiy, L. *et al.* Primate immunodeficiency virus proteins Vpx and Vpr counteract
961 transcriptional repression of proviruses by the HUSH complex. *Nat. Microbiol.* **3**, 1354–1361
962 (2018).
963 56. Lozzio, C. B. & Lozzio, B. B. Human Chronic Myelogenous Leukemia Cell-Line With Positive
964 Philadelphia Chromosome. *Blood* **45**, 321–334 (1975).
965 57. Zhao, L.-J., Mukherjee, S. & Narayan, O. Biochemical mechanism of HIV-I Vpr function.
966 Specific interaction with a cellular protein. *J. Biol. Chem.* **269**, 15577–15582 (1994).
967 58. DeHart, J. L. *et al.* HIV-1 Vpr activates the G2 checkpoint through manipulation of the
968 ubiquitin proteasome system. *Virol. J.* **4**, 57 (2007).
969 59. Lu, J., Pan, Q., Rong, L., Liu, S.-L. & Liang, C. The IFITM Proteins Inhibit HIV-1 Infection. *J.*
970 *Virol.* **85**, 2126–2137 (2011).
971 60. Compton, A. A. *et al.* IFITM Proteins Incorporated into HIV-1 Virions Impair Viral Fusion and
972 Spread. *Cell Host Microbe* **16**, 736–747 (2014).

973 61. Mashiba, M., Collins, D. R., Terry, V. H. & Collins, K. L. Vpr overcomes macrophage-specific
974 restriction of HIV-1 Env expression and virion production. *Cell Host Microbe* **16**, 722–735
975 (2014).
976 62. Kumar, H., Kawai, T. & Akira, S. Toll-like receptors and innate immunity. *Biochem. Biophys.*
977 *Res. Commun.* **388**, 621–625 (2009).
978 63. Deletsu, S. D. *et al.* Identification and characterization of Stathmin 1 as a host factor
979 involved in HIV-1 latency. *Biochem. Biophys. Res. Commun.* **567**, 106–111 (2021).
980 64. Park, G.-H. *et al.* Association between Interferon-Inducible Protein 6 (IFI6) Polymorphisms
981 and Hepatitis B Virus Clearance. *Genomics Inform.* **11**, 15–23 (2013).
982 65. Del Cornò, M. *et al.* HIV-1 gp120 signaling through TLR4 modulates innate immune
983 activation in human macrophages and the biology of hepatic stellate cells. *J. Leukoc. Biol.*
984 **100**, 599–606 (2016).
985 66. Okumura, A., Lu, G., Pitha-Rowe, I. & Pitha, P. M. Innate antiviral response targets HIV-1
986 release by the induction of ubiquitin-like protein ISG15. *Proc. Natl. Acad. Sci.* **103**, 1440–
987 1445 (2006).
988 67. Tartour, K. *et al.* Interference with the production of infectious viral particles and bimodal
989 inhibition of replication are broadly conserved antiviral properties of IFITMs. *PLOS Pathog.*
990 **13**, e1006610 (2017).
991 68. Yu, J. *et al.* IFITM Proteins Restrict HIV-1 Infection by Antagonizing the Envelope
992 Glycoprotein. *Cell Rep.* **13**, 145–156 (2015).
993 69. Cull, A. H., Snetsinger, B., Buckstein, R., Wells, R. A. & Rauh, M. J. Tet2 restrains
994 inflammatory gene expression in macrophages. *Exp. Hematol.* **55**, 56-70.e13 (2017).
995 70. Lorsbach, R. B. *et al.* TET1, a member of a novel protein family, is fused to MLL in acute
996 myeloid leukemia containing the t(10;11)(q22;q23). *Leukemia* **17**, 637–641 (2003).
997 71. Lang, S. M. *et al.* Importance of vpr for infection of rhesus monkeys with simian
998 immunodeficiency virus. *J. Virol.* **67**, 902–912 (1993).
999 72. Munde, M. *et al.* Structure-dependent inhibition of the ETS-family transcription factor PU.1
1000 by novel heterocyclic diamidines. *Nucleic Acids Res.* **42**, 1379–1390 (2014).

1001 73. McNamara, L. A., Ganesh, J. A. & Collins, K. L. Latent HIV-1 infection occurs in multiple
1002 subsets of hematopoietic progenitor cells and is reversed by NF-κB activation. *J. Virol.* **86**,
1003 9337–50 (2012).
1004 74. Norrander, J., Kempe, T. & Messing, J. Construction of improved M13 vectors using
1005 oligodeoxynucleotide-directed mutagenesis. *Gene* **26**, 101–106 (1983).
1006 75. Carter, C. C. *et al.* HIV-1 infects multipotent progenitor cells causing cell death and
1007 establishing latent cellular reservoirs. *Nat. Med.* **16**, 446–451 (2010).
1008 76. Weber, K., Bartsch, U., Stocking, C. & Fehse, B. A multicolor panel of novel lentiviral 'gene
1009 ontology' (LeGO) vectors for functional gene analysis. *Mol. Ther. J. Am. Soc. Gene Ther.* **16**,
1010 698–706 (2008).
1011 77. Moffat, J. *et al.* A Lentiviral RNAi Library for Human and Mouse Genes Applied to an Arrayed
1012 Viral High-Content Screen. *Cell* **124**, 1283–1298 (2006).
1013 78. Sarbassov, D. D., Guertin, D. A., Ali, S. M. & Sabatini, D. M. Phosphorylation and Regulation
1014 of Akt/PKB by the Rictor-mTOR Complex. *Science* **307**, 1098–1101 (2005).
1015 79. Wickham, H. *ggplot2*. (Springer, 2009). doi:10.1007/978-0-387-98141-3.
1016 80. Heinz, S. *et al.* Simple Combinations of Lineage-Determining Transcription Factors Prime cis-
1017 Regulatory Elements Required for Macrophage and B Cell Identities. *Mol. Cell* **38**, 576–589
1018 (2010).
1019 81. Eden, E., Navon, R., Steinfeld, I., Lipson, D. & Yakhini, Z. GOrilla: a tool for discovery and
1020 visualization of enriched GO terms in ranked gene lists. *BMC Bioinformatics* **10**, 48 (2009).
1021 82. Eden, E., Lipson, D., Yogev, S. & Yakhini, Z. Discovering Motifs in Ranked Lists of DNA
1022 Sequences. *PLOS Comput. Biol.* **3**, e39 (2007).
1023 83. Supek, F., Bošnjak, M., Škunca, N. & Šmuc, T. REVIGO Summarizes and Visualizes Long Lists
1024 of Gene Ontology Terms. *PLOS ONE* **6**, e21800 (2011).
1025 84. Kent, W. J. *et al.* The Human Genome Browser at UCSC. *Genome Res.* **12**, 996–1006 (2002).
1026 85. Grant, C. E., Bailey, T. L. & Noble, W. S. FIMO: scanning for occurrences of a given motif.
1027 *Bioinformatics* **27**, 1017–1018 (2011).
1028 86. Hao, Y. *et al.* Integrated analysis of multimodal single-cell data. *Cell* **184**, 3573-3587.e29
1029 (2021).

1030 87. RStudio Team. RStudio: Integrated Development for R. (2020).
1031 88. Gasmi, M. *et al.* Requirements for Efficient Production and Transduction of Human
1032 Immunodeficiency Virus Type 1-Based Vectors. *J. Virol.* **73**, 1828–1834 (1999).
1033

Supplemental Table 1

			Percent Infected	
Donor	Experiment Type	Molecule	89.6 WT vpr	89.6 vpr-null
1	Flow Cytometry	Protein	65%	50%
1	scRNA-seq	mRNA	71%	48%
2	Flow Cytometry	Protein	45%	31%
2	scRNA-seq	mRNA	53%	28%
3	Flow Cytometry	Protein	52%	35%
3	scRNA-seq	mRNA	N/A	(a) 42%
3	scRNA-seq	mRNA	N/A	(b) 54%

Supplemental Table 1. MDM infection rates measured with Gag. Percent infection of 89.6^{wt} and $89.6^{\Delta vpr}$ infected MDMs from each of three donors was determined by quantifying the percent Gag+ cells by either flow cytometry (protein) or gene expression levels from scRNA-seq data (mRNA), as indicated by the experiment type and molecule, over the total number of cells analyzed.

Supplemental Figure 1

ETS Family Transcription Factors

Motif	TF Name	q-value	# Targets w/ Sequence
ACCGGAAGTG	ETV4	0.0000	1270
AACCGGAAGT	ETV1	0.0000	1228
ACAGGAAGTG	ETS1	0.0000	987
CACTTCCGGT	Fli1	0.0000	1229
CACTTCCGGT	Elk4	0.0000	1038
ACTTCCTGTT	Elf4	0.0000	930
CACTTCCGGT	Elk1	0.0000	1013
ACAGGAAGTG	ERG	0.0000	1135
AACCGGAAGT	GABPA	0.0000	995
AACCGGAAGT	ELF1	0.0000	925
ACCAGGAAGT	EHF	0.0000	876
AACCGGAAGT	ETS	0.0000	674
ACGAGGAAGT	ELF5	0.0000	557
CCACTTCCTGTT	Etv2	0.0000	768
ATTTCCTGTG	EWS	0.0001	327
AGAGGAAGTG	PU.1	0.0005	316
ACCAGGAAGT	ELF3	0.0011	417
AAAGAGGAAGTG	SpiB	0.0038	180
AACAGGAAAT	EWS:FLI1-fusion	0.0063	534
ACAGGATGTGGT	ETS:RUNX	0.0082	121
ACATCCTGGT	SPDEF	0.0121	624

Homeobox Family Transcription Factors

Motif	TF Name	q-value	# Targets w/ Sequence
CCCATAAAAC	Hoxa13	0.0043	647
TTTTATTGCG	HOXB13	0.0183	292
ACCATAAAA	Hoxd13	0.0183	1
AAGCACTTAA	Nkx3.1	0.0255	746
GGCAATAAAA	Hoxa9	0.0355	796

bZIP Family Transcription Factors

Motif	TF Name	q-value	# Targets w/ Sequence
CGGTGACGTCAC	CRE	0.0000	385
GATGACGTCA	Atf1	0.0043	434
AAATGACGTCAT	CREB5	0.0632	203

NRF Family Transcription Factors

Motif	TF Name	q-value	# Targets w/ Sequence
CTGCGCATGCGC	NRF1	0.0000	544
GTGCGCATGCGC	NRF	0.0003	1

CCAAT Family Transcription Factors

Motif	TF Name	q-value	# Targets w/ Sequence
AGCCAATCGG	NFY	0.0000	782

ETS/IRF Family Transcription Factors

Motif	TF Name	q-value	# Targets w/ Sequence
CGGAAGTGAAAC	PU.1-IRF	0.0004	670

IRF Family Transcription Factors

Motif	TF Name	q-value	# Targets w/ Sequence
GGAAGTGAAAGT	IRF8	0.0006	209
GAAAGTGAAAGT	IRF2	0.0049	75
GAAAGTGAAAGT	IRF1	0.0453	68
ACTTTCGTTTCT	T1ISRE	0.0504	8

ZF Transcription Factors

Motif	TF Name	q-value	# Targets w/ Sequence
AGTGGGCGGAGC	Sp5	0.0000	1786
CGGCCCCGCCCC	Sp2	0.0000	2047
GGGGGCGGGGCT	KLF1	0.0000	1607
GGCCCCGCCCCC	Sp1	0.0000	1125
AGGGTGTGGC	KLF5	0.0000	1787
TGGCCCCACCCTCGC	KLF3	0.0000	1089
CAAGATGGCGGC	YY1	0.0000	203
CTGGGCGTGGCC	KLF6	0.0000	1497
GGTGGGCGGGGC	KLF14	0.0000	2044
GCCACGCCCACT	Klf9	0.0001	780
GGGGGGGG	Maz	0.0012	1644
GCCACACCCA	Klf4	0.0056	531
AACTACAATTCCCAGAATGC	GFY	0.0183	200
ATTTCCCAGAATGCCT	ZNF143|ST	0.0567	275

bHLH Family Transcription Factors

Motif	TF Name	q-value	# Targets w/ Sequence
CCGGTCACGTGA	E-box	0.0000	212
GTCACGTGAC	Usf2	0.0000	290
GTCATGTGAC	MITF	0.0000	505
GTCACGTGACCC	TFE3	0.0000	160
GTCACGTG	CLOCK	0.0000	402
GGTCACGTGA	USF1	0.0002	371
ACCACGTG	c-Myc	0.0006	495
GCACGTGACC	bHLHE41	0.0036	888
GCACGTGCCT	bHLHE40	0.0041	280
GTCACGTG	BMAL1	0.0043	679
GACCACGTGG	n-Myc	0.0150	432
ACCACGTGGTCT	Max	0.0228	347
TACCACGTG	NPAS	0.0254	612
GCACGTACCC	HIF2a	0.0636	246

THAP Family Transcription Factors

Motif	TF Name	q-value	# Targets w/ Sequence
GACTACAACTCCCAGAAGGC	Ronin	0.0227	185

Supplemental Figure 1. Transcription factors and their predicted binding motifs in downregulated genes in MDMs expressing Vpr. Motifs, transcription factor names, significance (FDR q-value), and number of target genes identified by HOMER analysis of genes downregulated in the presence of Vpr (Figure 1E) from several transcription factor families.

Supplemental Figure 2

MCR1 promoter has both predicted and known PU.1 binding motifs

-500

AGAAAGGCTCTAAGCACTGAATGTGGAAACTGAAGGGGATGAGCTTCAACTCTGAAGTGTTTCCAGCGTAAAACT
GTCCTTTCCAGGGCCCGTGTGGCTGTCACTTCAGAGTGGAGGTTGTCTGCTGAGGGACCCCTGACTCAGCTGC
TTCCCAGGGGAAGCTCCGTCTTCCGGCACAGGTAATGGCCTGCAGCTTGATCTCCACCCAGCCCCATCTGAGCA
GGCCGGGAGCTCCCAGGCTGTTTCACTTCTCTCCTTCCTGACTCCTCACCATCACCATCGCCCTCTCTCCTCCC
CACCCCGCCACTCCTCTCCCACACGTGTCCCTTTCTCCCCTTCCTCTGCGTCTGCTCTTCTCAGAAGTTAGCTTA
CGAAGCAAAGTTGTTACTTTGAATTCCTGTTTTTCCAGCCACCCTCATGTGACAGGATGTCTCCTCAGTAGAGGCT
TTCCCTAAATTCAGGAGCCCTTTAAAAGGGAGGGCTTCCTCTGTAGTTCTTTTCAGCTGGGCAGCTCTGGGAACT
TGGATTAGGTGGAGAGGCAGTTGGGGGGCCTCGTTGTTTTGCGTCTTAGTTCCGCCCTCCTGTCCATCAGGAGA
AGGAAAGGATAAACCCTGGGCCATG

+1

PU.1 Binding Motif | TATA Box | 5'UTR | Start Codon

Supplemental Figure 2. The *MRC1* promoter contains multiple PU.1 binding motifs. The first 500 bp upstream of the start codon in *MRC1*, the gene that codes for mannose receptor. Previously reported PU.1 binding motifs are outlined in red. The double-box PU.1 motif was identified through inputting the HOMER generated PU.1 motif parameters into FIMO (Find Individual Motif Occurrences). The TATA box is outlined in blue, the 5'UTR in yellow, and the start codon in green.

Supplemental Figure 3

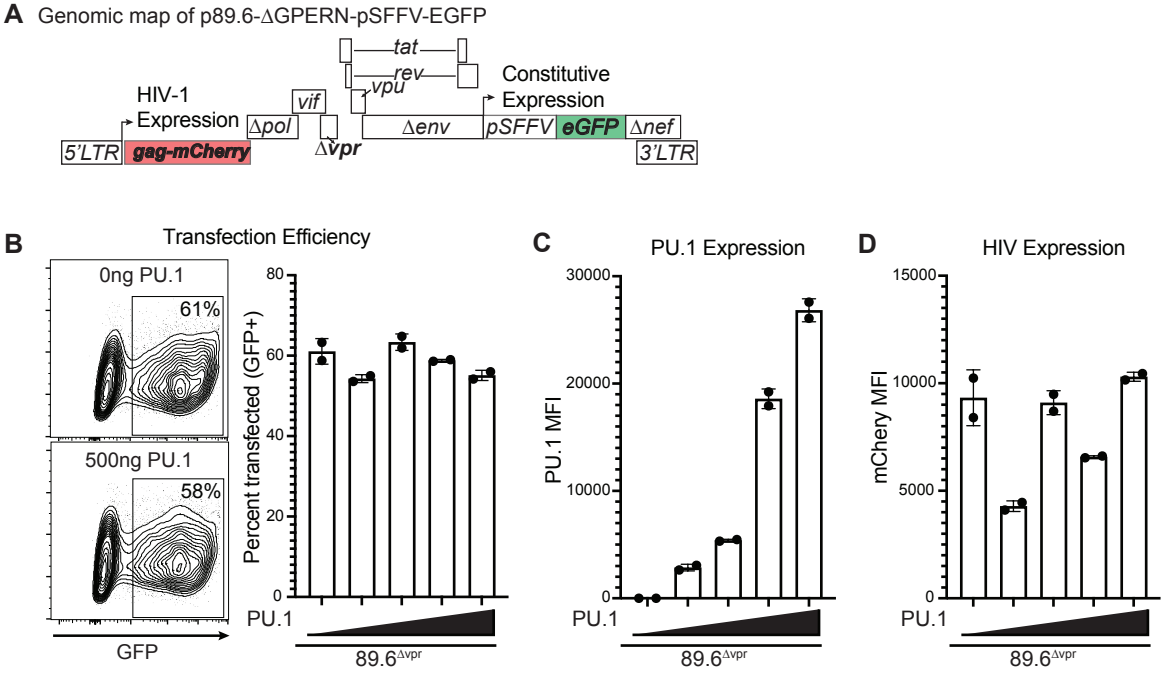

Supplemental Figure 3. PU.1 does not alter HIV-LTR activity. (A) Genomic map for 89.6-derived HIV-1 fluorescent reporter virus (89.6-ΔGPERN-pSFFV-EGFP). (B) Representative flow plots and bar graph assessing transfection rate via GFP expression in HEK 293T cells transfected with the indicated amount of PU.1 construct from Figure 2E plus 500ng of 89.6-ΔGPERN-pSFFV-EGFP from (A). (C) Summary graph of PU.1 expression in GFP$^+$ cells from (B). PU.1 levels were assessed using intracellular staining as described in Methods and measured by flow cytometry. (D) Summary graph of HIV-LTR activity as assessed by mCherry MFI from the same cells as in (C), measured flow cytometrically. All conditions were transfected with 500ng of HIV expression plasmid plus 0, 1, 10, 100, or 500ng of PU.1 plasmid. MFI = mean fluorescence intensity.

Supplemental Figure 4

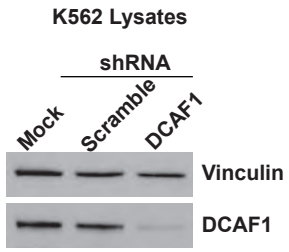

Supplemental Figure 4. DCAF1 protein is reduced in K562 cells via shRNA. Immunoblot of lysates from K562 cells stably transduced with virus expressing a non-targeting shRNA (shScramble) or one targeting DCAF1 (shDCAF1) compared to un-transduced cells (Mock).